IFM-GEOMAR REPORT

IFM-GEOMAR

Leibniz-Institut für Meereswissenschaften
an der Universität Kiel

FS Poseidon
Fahrtbericht / Cruise Report P362-2

West Nile Delta Mud Volcanoes

Piräus - Heraklion
09.02. - 25.02.2008

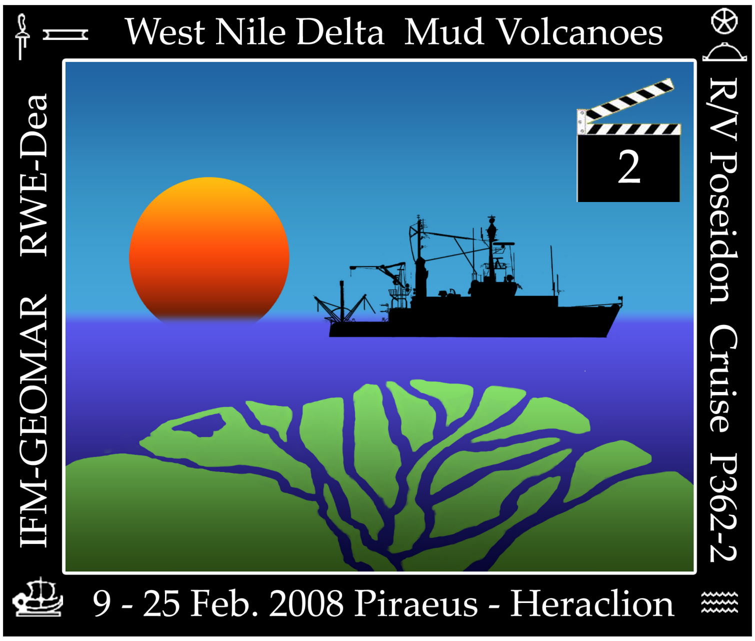

Berichte aus dem Leibniz-Institut
für Meereswissenschaften an der
Christian-Albrechts-Universität zu Kiel

Nr. 15
Mai 2008

IFM-GEOMAR
Leibniz-Institut für Meereswissenschaften
an der Universität Kiel

FS Poseidon
Fahrtbericht / Cruise Report P362-2

West Nile Delta Mud Volcanoes

Piräus - Heraklion
09.02. - 25.02.2008

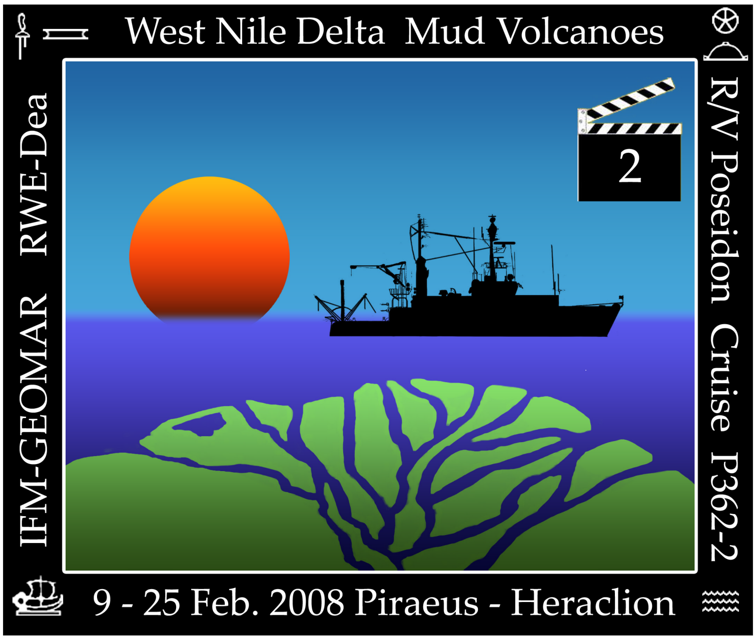

Berichte aus dem Leibniz-Institut
für Meereswissenschaften an der
Christian-Albrechts-Universität zu Kiel

Nr. 15, Mai 2008

ISSN Nr.: 1614-6298

IFM-GEOMAR
Leibniz-Institut für Meereswissenschaften
an der Universität Kiel

Das Leibniz-Institut für Meereswissenschaften ist ein Institut der Wissenschaftsgemeinschaft Gottfried Wilhelm Leibniz (WGL)

The Leibniz-Institute of Marine Sciences is a member of the Leibniz Association (Wissenschaftsgemeinschaft Gottfried Wilhelm Leibniz).

Herausgeber / Editor:
Tomas Feseker

IFM-GEOMAR Report
ISSN Nr.: 1614-6298

Leibniz-Institut für Meereswissenschaften / Leibniz Institute of Marine Sciences
IFM-GEOMAR
Dienstgebäude Westufer / West Shore Building
Düsternbrooker Weg 20
D-24105 Kiel
Germany

Leibniz-Institut für Meereswissenschaften / Leibniz Institute of Marine Sciences
IFM-GEOMAR
Dienstgebäude Ostufer / East Shore Building
Wischhofstr. 1-3
D-24148 Kiel
Germany

Tel.: ++49 431 600-0
Fax: ++49 431 600-2805
www.ifm-geomar.de

Preface

The research cruise P362/2 of *R/V Poseidon* was the second cruise to the western Nile deep-sea fan in the framework of the West Nile Delta Project at IFM-GEOMAR, generously supported by RWE-Dea.

Although this cruise was characterized by challenging weather conditions, we were all very satisfied with what was accomplished during those two weeks at sea. Both periods of good weather were used to full advantage. This achievement is not only due to the Captain's reliable weather forecasts but also to the outstanding efforts of the deck crew, supervised by Achim Mischker, the boatswain. It is sure that this cruise would not have been as successful without the tireless deck work of Pedro Tito, Jürgen Sauer, Bernd Rauh, Ronald Kuhn and Thomas Oberschelp . We are grateful for making it possible to obtain a large amount of samples and data that will keep us busy back in Kiel for quite some time.

On behalf of all cruise participants I would like to thank Captain Michael Schneider and the entire crew for the successful cruise. The friendly atmosphere on board and the good support of our work make this cruise a memorable one, and we are looking forward to our next cruise on *R/V Poseidon*.

Naturally, the preparations for this expedition started long before *R/V Poseidon* left the port of Piraeus. In fact, Warner Brückmann had already accomplished most of the work when preparing the previous cruise, so P362/2 profited from the excellent planning of P362, but I doubt that a single piece of equipment would have reached the vessel on time without Silke Schenck, who kept an overview of the logistics and also translated the daily weblog to English in real-time. Last not least, I would like to acknowledge Mr. Gamal Kassem of RWE Egypt for his valuable support.

Kiel, April 2008

Tomas Feseker

Contents

List of Figures

List of Tables

Chapter 1

Introduction

Tomas Feseker

1.1 Objectives of the cruise

Submarine mud volcanoes have been discovered all over the world on both active and passive margins (Kopf, 2002). Fluid formation and fluidization processes occuring at depths of several kilometers below the sea floor are driving complex systems of geochemical, geological and microbial processes. As mud volcanoes act as natural leakages for oil and gas reservoirs, these near-surface phenomena can be used for monitoring processes that occur at great depth. Detailed studies have shown that most mud volcanoes are associated with unique ecosystems often fueled by methane seepage (e.g. Werne et al., 2004; de Beer et al., 2006). Even though microbial communities act as a filter (Niemann et al., 2006), it has been shown that methane emitted from mud volcanoes reaches the mixing layer in the upper water column (Sauter et al., 2006). To quantify the role of mud volcanoes in global budgets, it is important to understand their activity (cf. Wallmann et al., 2006). Despite the fact that some mud volcanoes such as the Håkon Mosby mud volcano on the Barents Sea slope have been investigated for years, their functioning is still poorly understood and little is known about temporal variations of mud volcano activity (Feseker et al., 2008).

Apparently rooted at depths of more than 5 kilometers, Giza mud volcano (Giza MV) and North Alex mud volcano (North Alex MV) are located in the immediate vicinity of designated gas production wells on the upper slope of the western Nile deep-sea fan (figure 1.1). In the framework of the West Nile Delta Project at IFM-GEOMAR, these two mud volcanoes were selected for detailed investigation aiming to provide new insights into the dynamics of these unique sea floor features and their relation to gas reservoirs.

The objectives of the research cruise P362/2 of *R/V Poseidon* were to detect and quantify seepage of pore fluids and gases, characterize the chemical and isotopic composition of pore fluids, identify light volatile hydrocarbon gases and organic biomarkers, and to determine the evolution and eruption history of the selected mud volcanoes. A heatflow probe was used for measurements of temperature and thermal conductivity in the upper sediments. A gravity corer and a multicorer were used to retrieve sediment cores for geochemical, sedimentological and micropalaeontological studies. The position of the devices at the seafloor was determined by means of a GAPS positioning system.

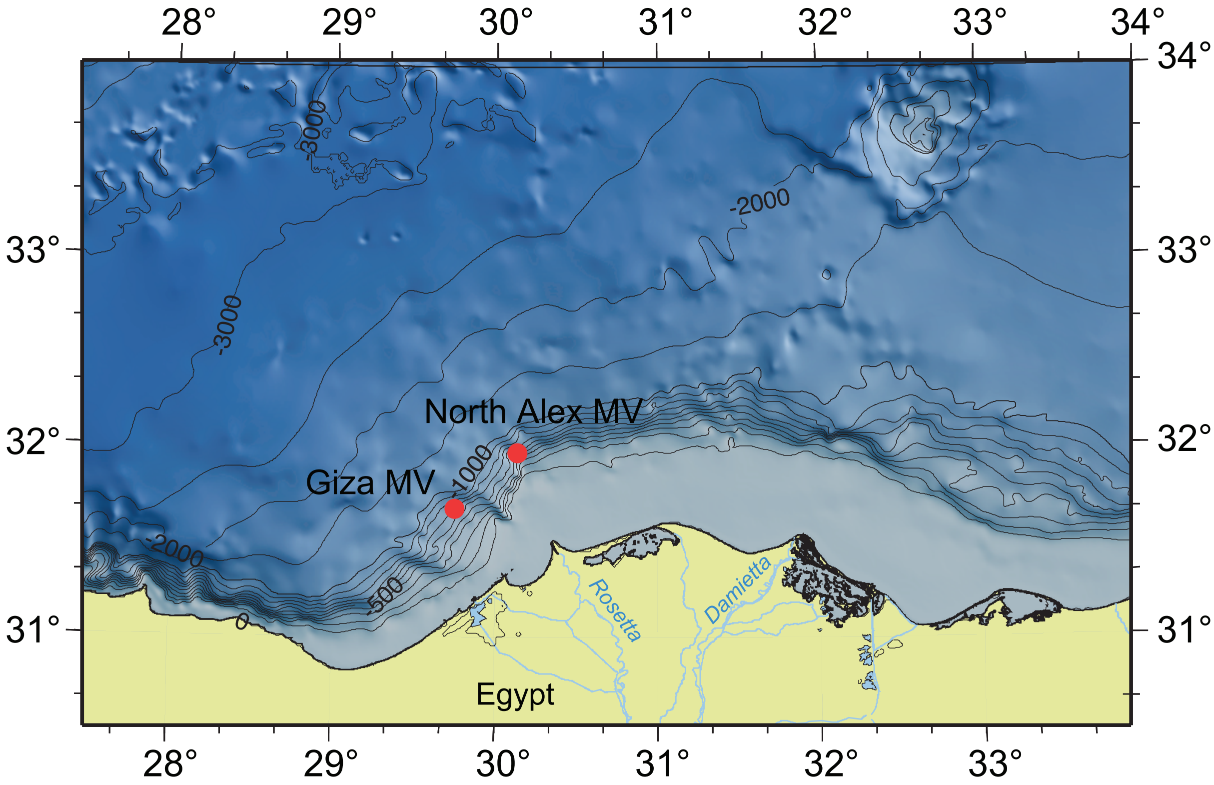

Figure 1.1: The mud volcanoes "Giza" and "North Alex" are located on the western Nile deep-sea fan at a distance of approximately 30 nm from the Egyptian coast.

1.2 Geological setting

The Nile deep-sea fan is the most important sedimentary accumulation in the eastern Mediterranean. Two geophysical mapping campaigns conducted in 1998 (Prismed II) and 2000 (Fanil) resulted in a first detailed morphostructural description of this deep-sea fan (Mascle et al., 2001; Loncke et al., 2002, 2004) and led to the discovery of several circular and sub-circular sedimentary structures on the upper slope. Up to a few kilometers in diameter and generally showing a low relief of a few tens of meters, these mud volcanoes or so-called 'mud pies' have been described as surface expressions of deep-seated gas chimneys (Loncke et al., 2002, 2004), which are related to faults and controlled by the tectonic regime (Dupre et al., 2007). Some of them are associated with large methane plumes in the water column (Mastalerz et al., 2007). For a detailed structural analysis of the Nile deep-sea fan, see Loncke et al. (2006).

1.3 Working areas

1.3.1 Giza MV

Giza MV is located at 31°40.51' N and 029°45.00' E at a water depth of around 700 m on the upper slope of the western Nile deep-sea fan. It is a circular structure of around 2500 m in diameter. The highest point of Giza MV, slightly SE of the geometrical center, is elevated approximately 40 m above the surrounding seafloor and forms a pronounced summit on an otherwise flat plateau on the top of the mud volcano. Figure 1.2 shows the microbathymetry of the working area. Additionally, the morphology is illustrated along selected transect lines in figure 1.3. NW of the central area, a gap in the moat surrounding the mud volcano points to gravity slides or outflow of mud.

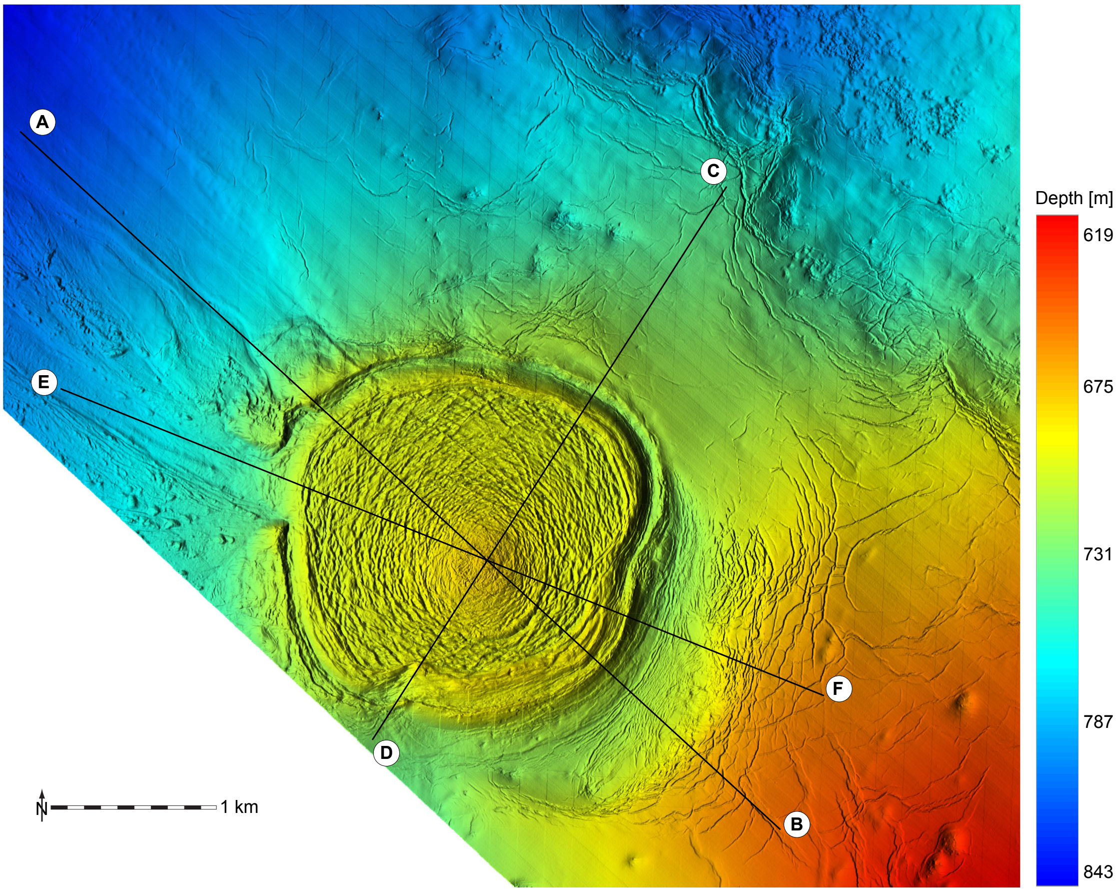

Figure 1.2: Shaded microbathymetric map of Giza MV. The boundaries of the map correspond to the boundaries of working area 1 as defined in the work permit issued by the Egyptian authorities. The microbathymetry along the black transect lines is shown in figure 1.3. (DTM courtesy of BP)

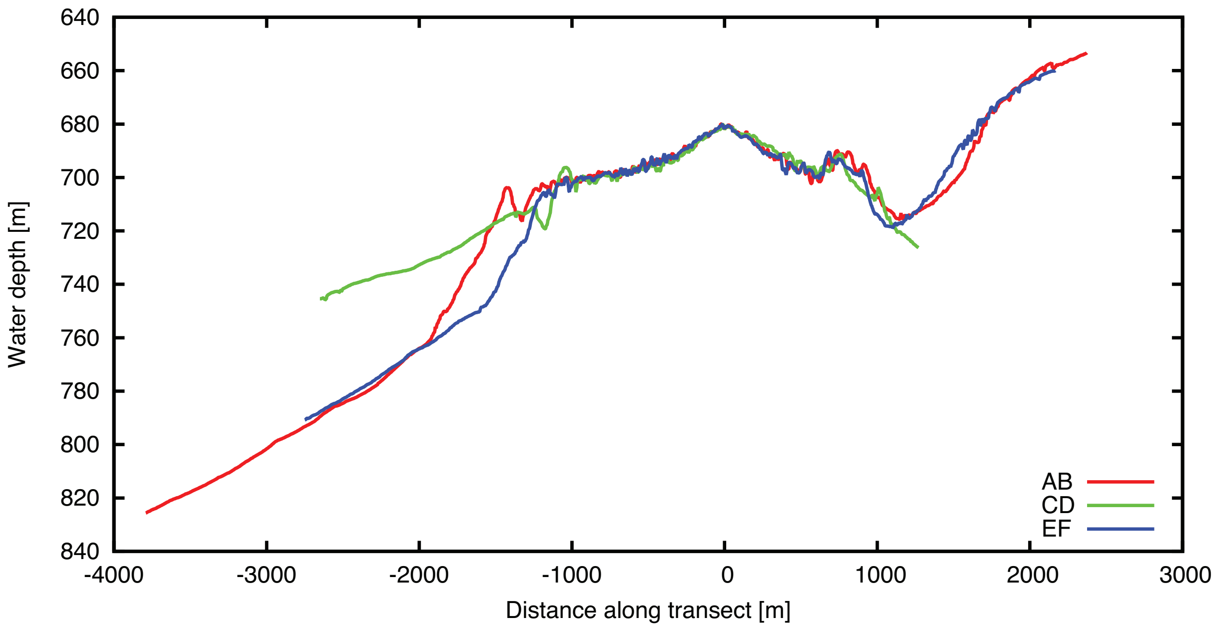

Figure 1.3: Microbathymetry along three transects across Giza MV. The location of the transect lines is shown in figure 1.2.

1.3.2 North Alex MV

North Alex MV is located at 31°58.19' N and 030°08.21' E at a water depth of around 500 m, approximatly 26 nm NE of Giza MV. It is a circular structure with a diameter of less than 2000 m and an elevation of nearly 50 m above the surrounding seafloor at its highest point. The central plateau is characterized by gentle slopes toward a steep edge of about 40 m. The microbathymetry of the working area (figure 1.4) suggests a series of slides due to slope failure or mud flows NNE of the central area. The mud volcano appears to be situated exactly at the transition between smooth seafloor upslope and seafloor altered by ripple-like structures and superficial faults downslope. In figure 1.5, the morphology of North Alex MV is illustrated along two microbathymetry transects.

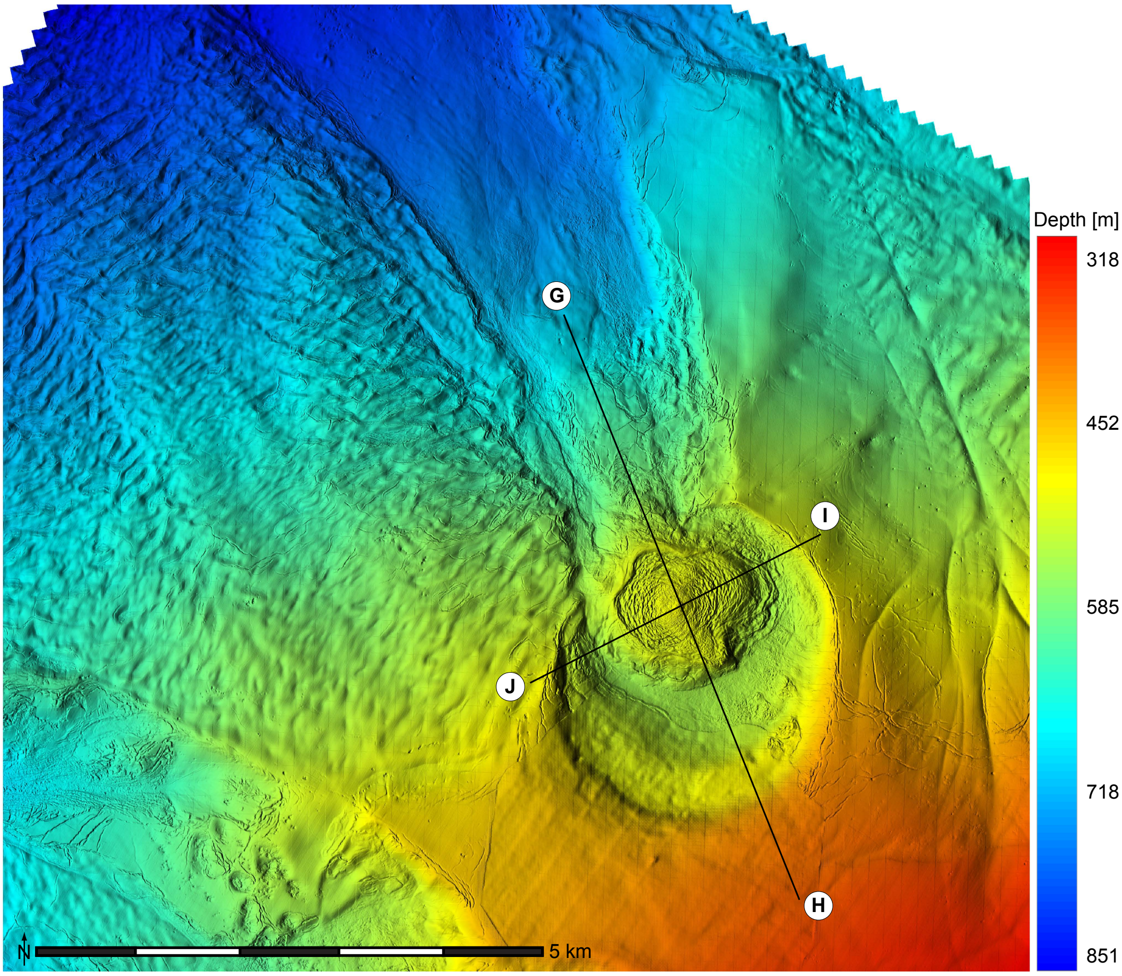

Figure 1.4: Shaded microbathymetric map of North Alex MV. The boundaries of the map correspond to the boundaries of working area 2 as defined in the work permit issued by the Egyptian authorities. The microbathymetry along the black transect lines is shown in figure 1.5. (DTM courtesy of BP)

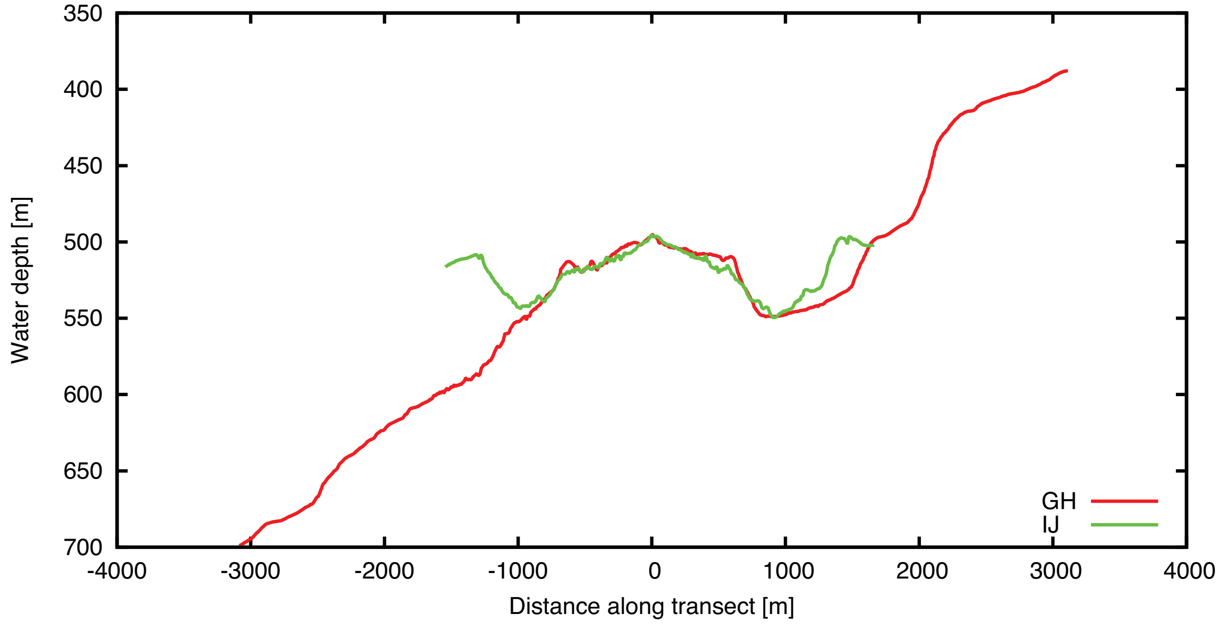

Figure 1.5: Microbathymetry along two transects across North Alex MV. The location of the transect lines is shown in figure 1.4.

Chapter 2

Cruise narrative

Tomas Feseker

The research cruise P362/2 of *R/V Poseidon* is the second expedition to the Nile deep-sea fan in the framework of the West Nile Delta Project at IFM-GEOMAR. As the previous research cruise P362, which took place in December 2007, had to be cancelled due to technical problems, the main motivation of the ten scientists onboard the vessel (figure 2.1) during this cruise was to complete the work that had been planned. The following is a brief summary of the work during the two weeks at sea. A more detailed report of the daily events is available from the Internet at `http://www.ifm-geomar.de/index.php?id=p362-2&L=1`.

Figure 2.1: The scientific party of P362/2: Wiebke Nehmiz, Gero Wetzel, Florian Scholz, Anke Bleyer, Tomas Feseker, Ahmed Kamal Naguib, Marianne Nuzzo, Regina Surberg, Kevin Brown, Janne Lorenzen, Thorsten Schott (from left to right).

Transit to the first working area, boarding of the Egyptian observer

R/V Poseidon left the port of Piraeus, Greece, on February 10. Due to severe weather conditions on the planned course to the Nile delta area, the departure of the vessel had been postponed by one and a half days. Despite a force eight storm and 3 m swell on the first day, the transit went according to plan and *R/V Poseidon* reached the first working area around Giza MV at 07:00 local time on February 13. Just when the station work was about to start, a call from Cairo announced that an Officer of the Egyptian Navy had boarded a shuttle boat to take him to *R/V Poseidon* in order to accompany the expedition as an official representative of the Egyptian authorities. In order to meet the shuttle boat at approximately 11 nm from the port of Alexandria, the preparations for the first station were cancelled and course was set for the agreed meeting point, where Lt Cdr Ahmed Kamal Naguib of the Egyptian Hydrographic Office in Alexandria boarded *R/V Poseidon* shortly after noon on February 13.

Station work in at Giza MV

Upon return to the first working area on the same afternoon, the station work was started without any further delay. After a CTD cast to record a sound velocity profile of the water column required for the calibration of the GAPS positioning system, the gravity corer was deployed at a reference station approximately 2.4 km NE of the center of Giza MV, in an area where the morphology of the seafloor does not appear to be influenced by the mud volcano (cf. figure 3.1). While the analyses of the first samples started in the laboratories of the research vessel, the heatflow probe was deployed for the first time to conduct temperature and thermal conductivity measurements along a first transect line across the central area of Giza MV. The transect had been planned to take until the next morning, but a low pressure system with thunderstorms and force nine wind gushes was approaching the working area faster than expected and led to a premature interruption of the station work already after the first measurement.

The severe weather conditions continued for nearly two days and did not permit any station work, except for a test of a GAPS transponder that revealed technical problems with the positioning system. In the afternoon of February 15, the gravity corer was deployed at the center of Giza MV. For all deployments of the gravity corer, three autonomous temperature loggers and a tilt meter were attached to the corer barrel in order to determine the thermal regime from which samples are taken and to facilitate the later integration of temperature data and geochemical analyses. Three other successful deployments of the gravity corer at two different target sites on the mud volcano followed until the evening, when the heatflow probe was deployed for the second time to resume the planned transect. As the weather conditions further improved, in-situ temperature profiles were measured at 19 stations until the next morning. On February 16, sediment sampling started with two deployments of the multicorer, to which a sensor for methane measurements in the water column had been attached. As the weather forecast announced the next low pressure system within less than 24 hours, the Captain and crew of *R/V Poseidon* agreed to work extra hours while the weather still permitted station work, which allowed us to complete another five successful stations of the gravity corer until the late evening. The work on the samples in the laboratories continued during the night. As predicted, the wind speed increased during the night, but one last gravity core from Giza MV could be taken in the early morning of February 17 before station work had to be interrupted once again to wait for better weather conditions.

Station work at North Alex MV

While the next low-pressure system with up to force 11 winds rendered life on board rather uncomfortable, it was decided to set course for the second working area around North Alex

MV in order to make sure to get at least a few samples and measurements from the second target. The transit of around 25 nm from Giza MV to North Alex MV only takes a few hours, but as the storm continued, the work could not be resumed until February 20, when the gravity corer could be deployed at the center of North Alex MV at dawn. Finally and just in time for the second working area, the GAPS system was working correctly, allowing for precise determination of the position of the devices at the seafloor. Three more gravity corers were recovered until the heatflow probe was deployed around lunchtime. After six stations, the temperature measurements were interrupted briefly for another gravity core, before completing another 22 stations until the next morning. On February 21, the multicorer and the gravity corer were each deployed three times, yielding a vast number of samples from all over North Alex mud volcano. During the night, the temperature measurements continued with another 24 closely-spaced stations in the central area of North Alex MV. In the morning of February 22, there was still time for two final gravity corer before the station work had to be terminated.

Departure of the Egyptian observer, transit to Heraklion

After the end of station work at 10:30 February 22, *R/V Poseidon* set course for a meeting with a shuttle boat outside the port of Ras-Al-Teen, close to Alexandria. The Egyptian observer Lt Cdr Ahmed Kamal Naguib was picked up from *R/V Poseidon* at around 15:30 and *R/V Poseidon* immediately started the transit to the port of Heraklion, as the next low pressure system was to reach the coast of Egypt shortly and the Captain wanted to complete as much of the way as possible while the good weather still prevailed. *R/V Poseidon* reached the port of Heraklion safely in the early afternoon of February 24, one day earlier than planned.

Chapter 3

Sediment sampling

Tomas Feseker

3.1 Sampling strategy

At both Giza and North Alex MVs, the selection of the sampling locations was based on the assumption that the activity of the mud volcanoes is focussed at their morphological centers. Targets were defined in the central areas and at varying distances and directions from the center, in order to verify the apparent axisymmetric structure of the mud volcano. Additional targets were chosen according to morphological irregularities such as superficial faults, slides, or apparent mudflows, as identified in the microbathymetry. To facilitate the integration of the results of sediment sampling and temperature measurements, all sampling sites are located on transect lines across the mud volcanoes along which thermal data was collected using the heatflow probe.

3.2 Giza MV

The sampling sites at Giza MV are located on three pre-defined transect lines across the center of the mud volcano. A map of the gravity corer and multicorer stations is shown in figures 3.1 and 3.2, respectively. The first transect line AB runs from undisturbed seafloor downslope from the mud volcano across the central area to undisturbed sediments upslope of the mud volcano. Three sites at increasing distances from the center and the center itself were selected as targets. The second transect line CD starts at the reference site NE of the mud volcano, crosses the center, and ends at a structure that looks like a fault on the SW' edge of the mud volcano. The reference site, a location on the NE' edge, and the fault were targets located on this transect line. The third transect runs from an area apparently affected by gravity sliding or mud flows, NW of the mud volcano, across the center towards undisturbed sediments SE of the mud volcano. Targets on this transect line were the so-called 'Giza Outflow' site downslope and another site NW of the center.

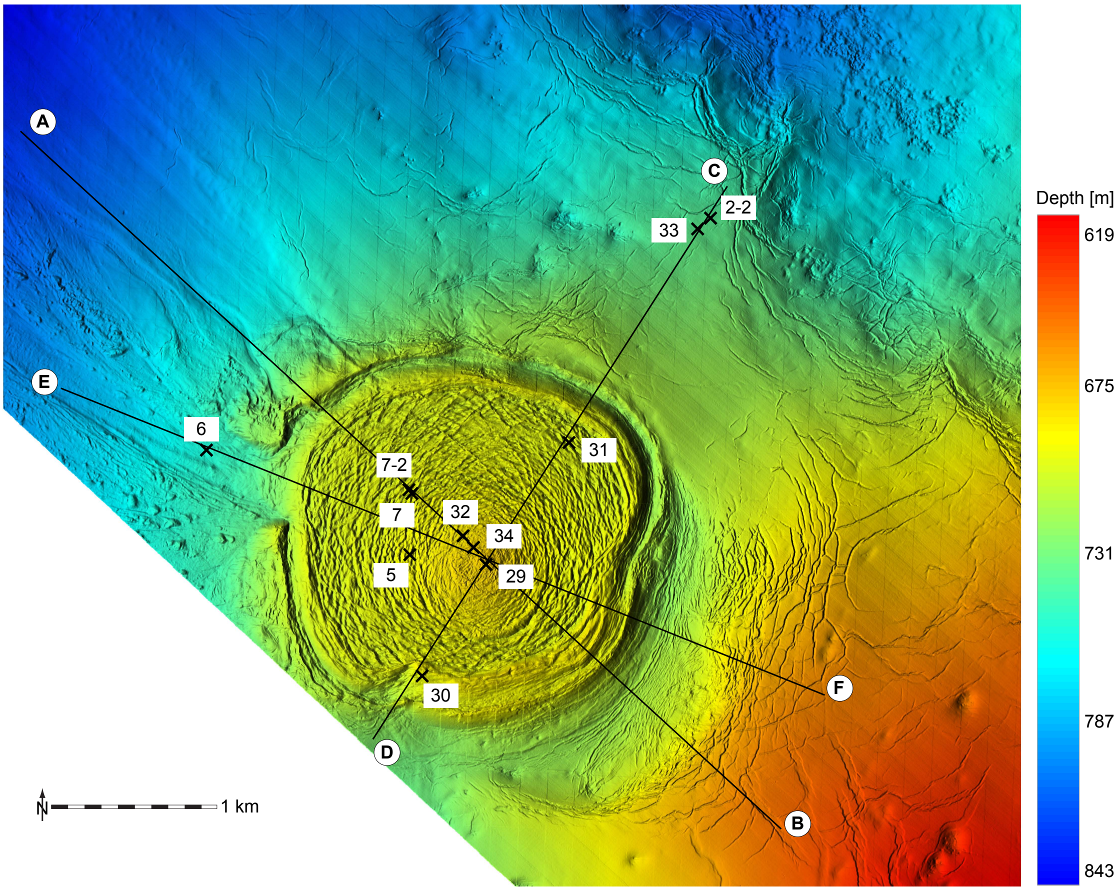

Figure 3.1: Gravity corer stations at Giza MV. (DTM courtesy of BP)

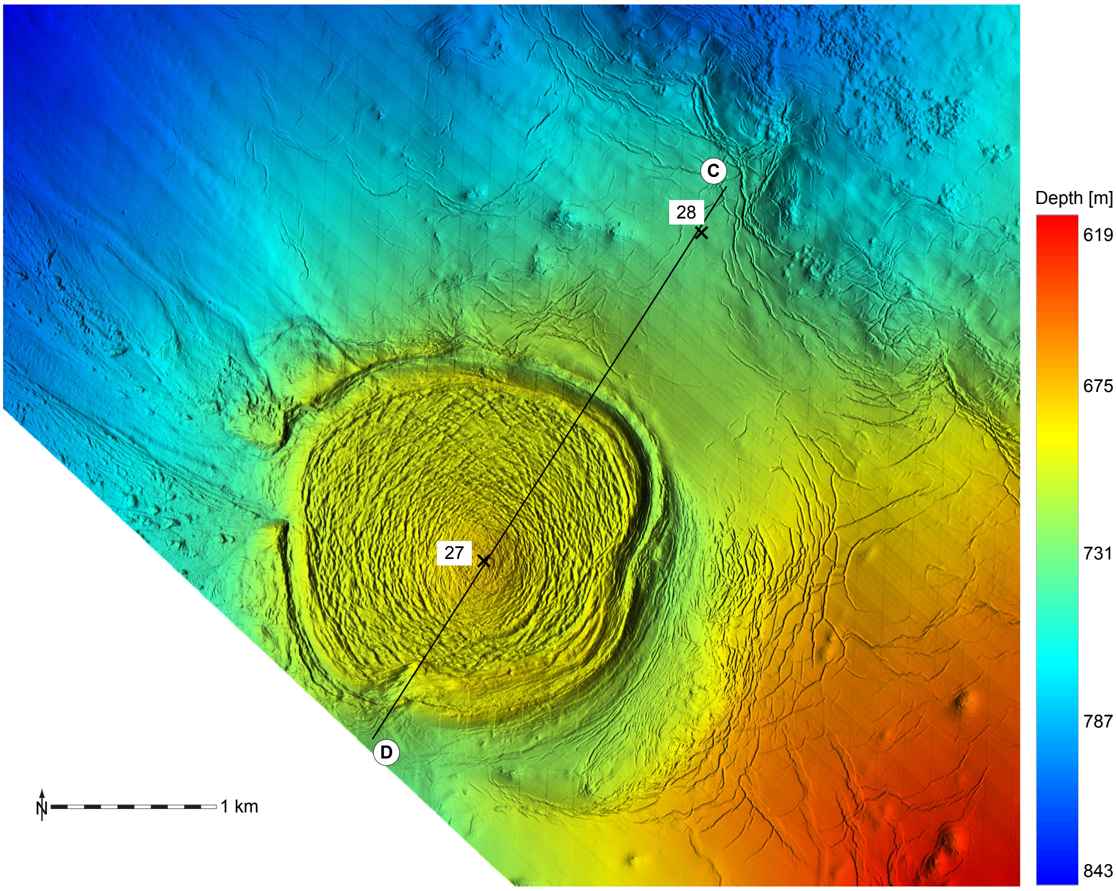

Figure 3.2: Multicorer stations at Giza MV. (DTM courtesy of BP)

3.3 North Alex MV

While the temperature measurements using the heatflow probe were conducted along two long perpendicular transect lines across the central area of North Alex MV (cf. figure 6.4), sediment samples were taken only in the center and on sites along a single transect due to limited time. Maps showing all stations of the gravity corer and the multicorer are given in figures 3.3 and 3.4, respectively. The transect line starts at a site named 'North Alex Far Outflow' in an area that appears to be strongly affected by gravity slides and/or mud flows downslope from the mud volcano. Crossing another 'Outflow' site closer to the mud volcano, the transect line continues towards a target on the plateau NW of the center, across the center itself and another site a short distance SE of the center. The line ends at a reference site upslope S of North Alex MV.

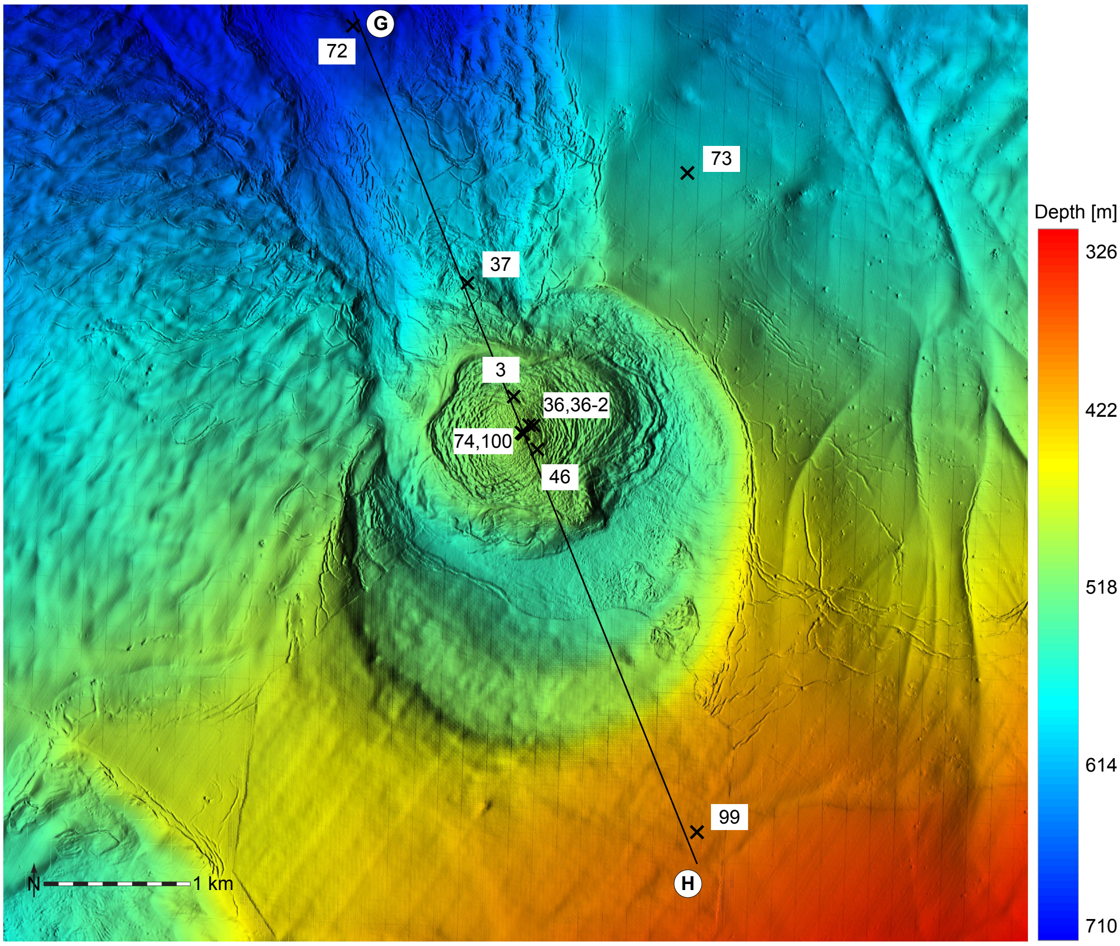

Figure 3.3: Gravity corer stations at North Alex MV. (DTM courtesy of BP)

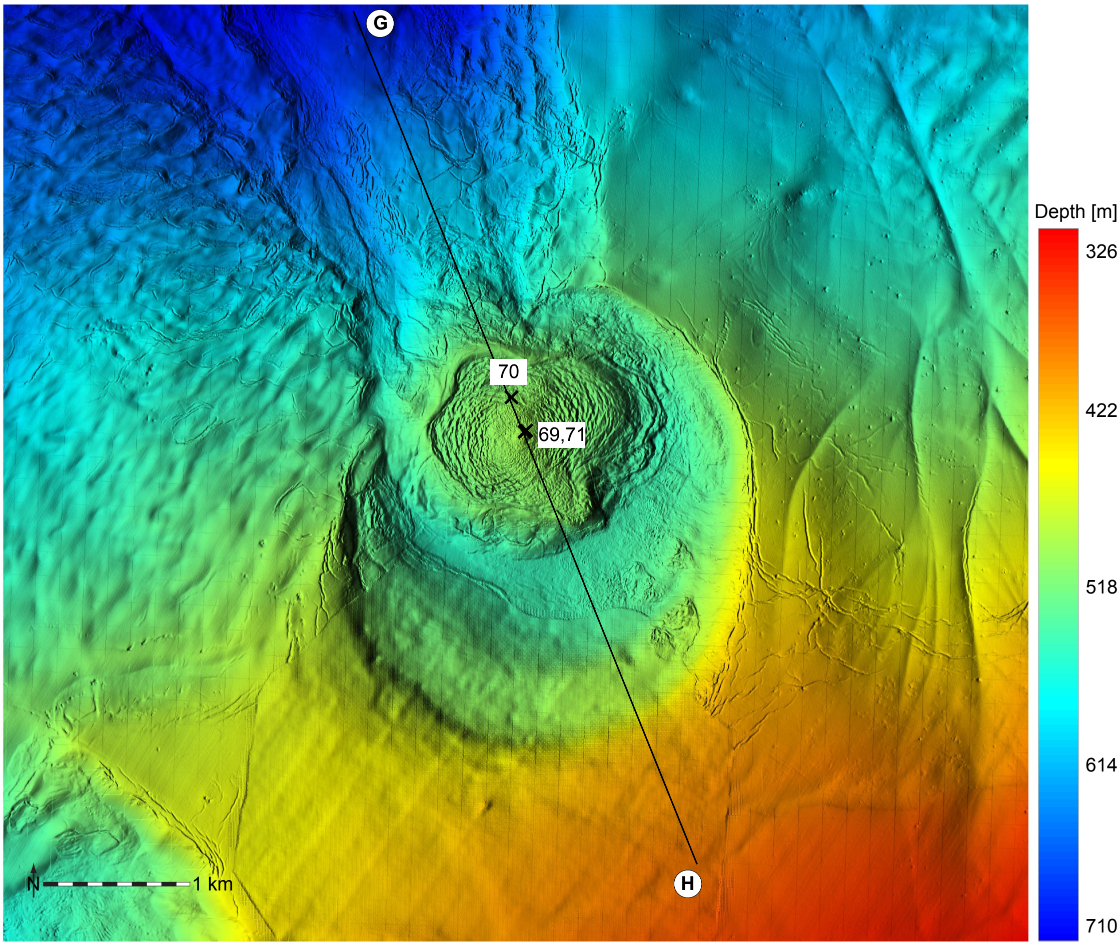

Figure 3.4: Multicorer stations at North Alex MV. (DTM courtesy of BP)

Chapter 4

Marine geochemistry

Marianne Nuzzo, Florian Scholz, Anke Bleyer, and Regina Surberg

4.1 Introduction

North Alex MV had been sampled previously, and unpublished data made available by Prof. Gert de Lange (University of Utrecht) suggested a thermogenic origin of hydrocarbon gases, and fluid geochemical signatures are pointing to a release of the fluids from deeply buried sediments. On the contrary, Giza MV had never been sampled previously and this constitutes the first data set regarding the geochemistry of fluids at this mud volcano. The aims of this study are (i) to constrain the deep origin of the fluids and hydrocarbons; (ii) to characterize the sources and thermal maturity of sedimentary organic matter; and (iii) to investigate the microbially-mediated reactions occurring in the shallow subsurface which lead to mineralization of vent hydrocarbons and recycling of major (e.g., Sulphur) and minor (e.g., Iron) elements yielding indications on past and present seep activity at the mud volcanoes. For this purpose, samples were recovered for the analysis of the inorganic and organic geochemistry of pore waters, of the isotopic geochemistry of light volatile hydrocarbon gases, and of sedimentary lipid biomarkers. The methodology applied to sampling and geochemical analyses performed on board are presented below, as well as an outline of the analyses which will be perfomed at shore-based laboratories. Preliminary results obtained onboard are also discussed thereafter.

4.2 Materials and methods

4.2.1 Sampling: sediment, pore water and gas recovery

Surface and subsurface sediment samples were retrieved using a gravity corer (GC) and multi-corer (MUC). For pore water recovery, the sediments of the MUCs were extruded stepwise and subsequently cut into 1 to 3 cm thick discs. The GCs were divided into 1 m sections and then cut lenghtwise into a work and an archive half. In the following, 2 - 5 cm thick sediment samples were taken in 15 - 40 cm intervals. Pore water recovery was done in a cooled lab at in-situ temperature (12 °C) using an argon gas pressure squeezer at 2 - 5 bars (Fig. 4.1a). While squeezing the pore water was filtered through cellulose acetate (0.45 μm) and acetate-free cellulose filters (0.2 μm) respectively. For Fe analyses the pore water was recovered under anoxic conditions using rhizone pore water samples (Fig. 4.1b) (obtained from Rhizosphere, the Netherlands). About 5 ml of each wet sediment slice was collected for porosity analyses. After squeezing the sediment samples were stored in plastic bags for geochemical analyses of the solid phase in shore-based labs. Most of the archive halves of the GCs and all water and sediment samples were stored cooled or refrigerated until further analysis. Pore water light volatile hydrocarbon gases were stripped from sediments according to the method of McAullife (1971) on sediments collected by MUC and GC. Sediment plugs were recovered using a 10 ml clean disposable polypropylene syringe that had the end cut off. The sediment plug was immediately injected in a 30 ml glass vial filled with 10 ml of 10% aqueous solution of potassium chloride (KCl). The vial was sealed and then vigorously shaken to disaggregate the mud and to stop all bacterial activity due to KCl poisoning (Bowes and Hornibrook, 2006). The sample was allowed to equilibrate with the vial headspace for 24 to 48 hours. The gas was extracted in a syringe by injecting an equivalent amount of 10% KCl solution. The headspace gas was later transferred into a 20 ml sterile serum vial filled (bubble-free) with a pH 1, 10% KCl solution by displacement of an equivalent amount of solution. The vials were stored upside down in order to minimize the potential for exchange with air through the septum. Sediments were also collected for analysis of lipid biomarkers. They were placed into furnaced glass vials and immeditaly stored at -20 °C for preservation and transport until analysis at the on-shore lab.

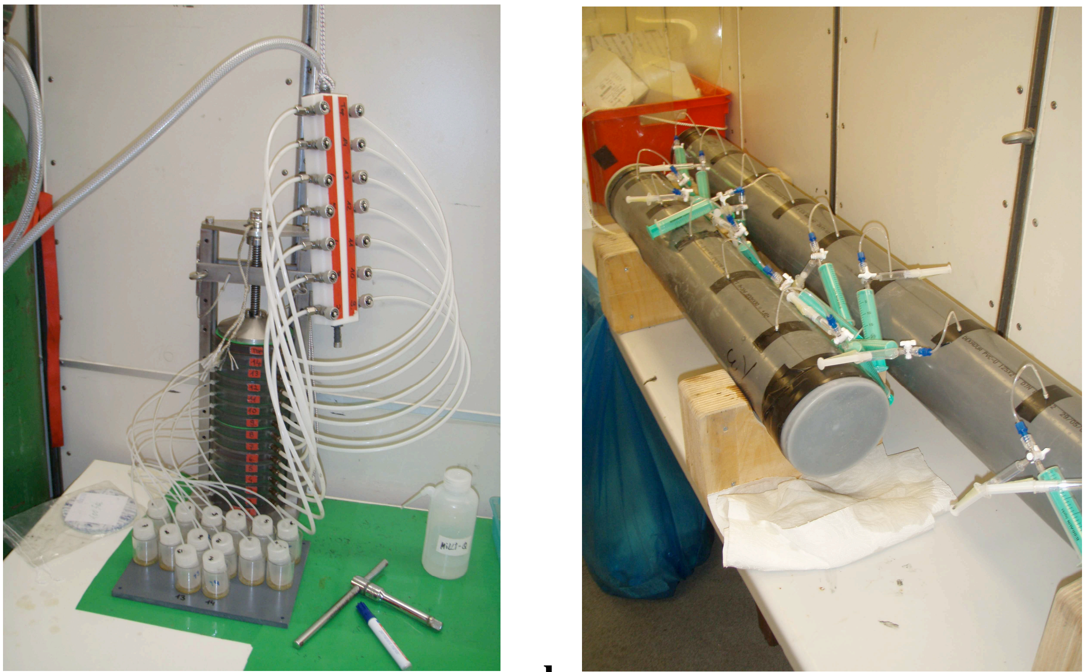

a **b**

Figure 4.1: Pore water pressure squeezer (a) and rhizon pore water samplers (b)

4.2.2 On-board chemical analyses

Analyses for the NH_4^+, PO_4^{3-}, SiO_4^{4-}, HS^- and Fe^{2+} were completed onboard using a Hitachi U2800A spectrophotometer. The respective chemical analytics follow standard procedures and are described in detail in Grasshoff et al. (1999) and on the IFM-GEOMAR webpage respectively. Since high sulfide contents (> 1 mM) interfere with the reactions of NH_4^+, PO_4^{3-}, and SiO_4^{4-}, these sub-samples were bubbled with argon for about 1 hour to strip any H_2S prior to the analysis. The total alkalinity (TA) of the pore water was determined by titration with HCl using the Tashiro indicator, a mixture of methyl red and methylene blue. The titration vessel was bubbled with nitrogen to strip any CO_2 and H_2S produced during the titration. Chloride concentrations were determined applying a Mohr titration with $AgNO_3$. The latter two methods were calibrated with IAPSO seawater standard.

4.2.3 Analyses at shore-based laboratories

Pore water sub-samples were taken for shore-based analyses of major and trace elements (ICP-AES, ICP-MS), anions (ion chromatography) and isotopes (H, O, Li, Cl, Sr). Leaching experiments and element analyses on the solid phase will be carried out on sediment samples or squeeze cakes. The molecular and stable carbon isotope composition of pore water Volatile Fatty Acids (VFAs) will be analyzed by High Performance Liquid Chromatography-pyrolysis-Mass spectrometry at the University of Bremen. The molecular (CH_4 to C_5H_{12}) and isotopic ($\delta^{13}C$-CH_4-C_5H_{12} and δD-CH_4) composition of light volatile hydrocarbon gases will be determined by Gas Chromatography (GC) and by GC-Combustion-Isotope Ratio Mass Spectrometry and GC-pyrolysis-IRMS. Lipid biomarkers will be extracted from the sediments, identified by GC-MS and quantified by GC, and the carbon isotopic composition of specific compounds will be estimated by GC-MS at the University of Bremen.

4.2.4 CH_4-Sensor

The Multicorer was deployed with an infrared methane sensor mounted above the liners (obtained from CONTROS, Germany) in order to measure CH_4 concentrations in the water column above the mud volcanoes (figure 4.2). The Sensor was equilibrated close to the sea surface for 15 minutes and then lowered up to 15 m above the sea floor. Measurements were carried out for 5 minutes both before and after the MUC had penetrated the sediments. The data which were recorded during the MUC deployments will be processed at IFM-GEOMAR after the cruise.

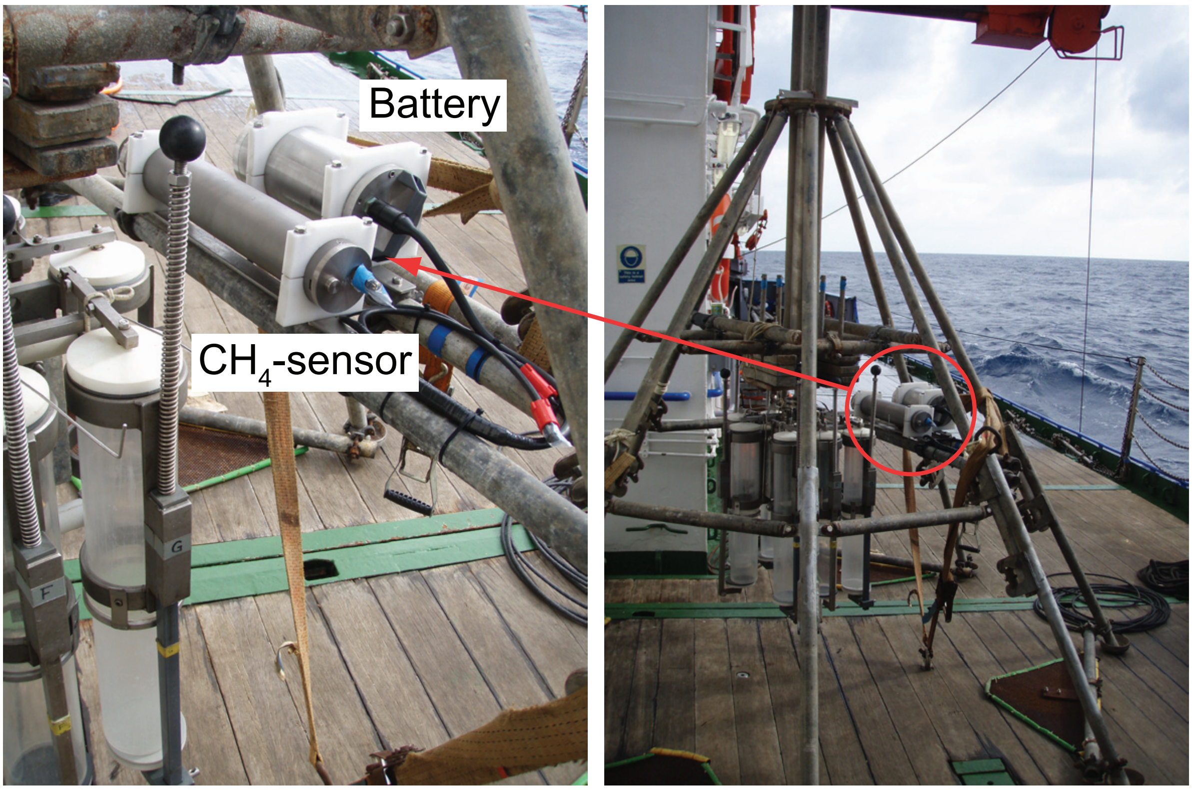

Figure 4.2: The CH_4-sensor was mounted on the frame of the multicorer.

4.3 Work at sea

During P362-2 the geochemistry group sampled and analyzed 12 GCs and 5 MUCs giving a total of 257 (inorganic geochemistry) and 188 (organic geochemistry) samples respectively. 1 GC and 1 MUC were taken at a reference site close to Giza MV in order to obtain geochemical data of hemipelagic Nile delta deep sea fan sediments which are not influenced by mud volcanism or fluid and gas seepage. The cores retrieved at Giza MV span a transect from the center at 675 m water depth (GC5, GC29, MUC27) to the NW slope (GC34, GC32, GC7). An additional core was taken at the SW slope (GC30). At North Alex MV 5 cores were retrieved at the center at 491 m water depth (GC36, GC74, GC100, MUC69, MUC71), 2 cores at the NW slope (GC38, MUC70) and 1 core at the SE slope (GC46). The CH_4-sensor was mounted on the frame of the multicorer and deployed four times, once at the reference site, once at the center of Giza and at the center of North Alex MVs and once at the NW of North Alex. An overview of the samples collected and the analyses that have been performed on-board is given in Tab. 4.1, 4.2, and 4.3.

Table 4.1: Inorganic geochemistry: list of pore water, sediment and gas sampling sites with on-board chemical analyses

Station	Site	Core length [cm]	Samples	TA	Cl^-	PO_4^{3-}	NH_4^+	SiO_4^{4-}	H_2S	Fe^{2+}
GC2	Reference	526	20	x	x	x	x	x	x	-
GC5	Giza center	296	13	x	x	x	x	x	x	-
GC7	Giza NW	340	14	x	x	x	x	x	x	-
MUC27	Giza center	34	20	x	x	x	x	x	x	-
MUC28	Reference	29	12	x	x	x	x	x	x	-
GC29	Giza center	121	8	x	x	x	x	x		-
GC30	Giza SW	492	12	x	x	x	x	x	x	-
GC32	Giza center/NW	268	13	x	x	x	x	x	x	-
GC34	Giza center/NW 2	420	19	x	x	-	x	x	x	-
GC36	North Alex center	271	16	x	x	x	x	x	x	-
GC38	North Alex NW	263	15	x	x	x	x	x	x	-
GC46	North Alex SE	276	14	x	x	x	x	x	x	-
MUC69	North Alex center	27	22	x	x	x	x	x	x	x
MUC70	North Alex NW	19	20	x	x	x	x	x	x	x
MUC71	North Alex center	31	14	-	-	-	-	-	x	-
GC74	North Alex center	294	14	x	x	x	x	x	x	x
GC100	North Alex center	264	11	x	x	x	x	x	x	-

Table 4.2: Inorganic geochemistry: list of pore water, sediment and gas sampling sites where subsamples for shore-based analyses were obtained

Station	Site	Core length [cm]	Samples	ICP-OES	ICP-MS	IC	$\delta^{18}O/\delta D$	$\delta^{13}C$	Sr-/Li-/Cl-Isotopes
GC2	Reference	526	20	x	-	x	x	x	x
GC5	Giza center	296	13	x	-	x	x	-	x
GC7	Giza NW	340	14	x	-	x	x	x	x
MUC27	Giza center	34	20	x	-	x	x	x	x
MUC28	Reference	29	12	x	-	x	x	x	x
GC29	Giza center	121	8	x	-	x	x	x	x
GC30	Giza SW	492	12	x	-	x	x	x	x
GC32	Giza center/NW	268	13	x	-	x	x	x	x
GC34	Giza center/NW 2	420	19	x	-	x	x	x	x
GC36	North Alex center	271	16	x	-	x	x	x	x
GC38	North Alex NW	263	15	x	-	x	x	x	x
GC46	North Alex SE	276	14	x	-	x	x	x	x
MUC69	North Alex center	27	22	x	x	x	x	x	x
MUC70	North Alex NW	19	20	x	x	x	x	x	x
MUC71	North Alex center	31	14	x	-	x	x	x	-
GC74	North Alex center	294	14	x	x	x	x	-	x
GC100	North Alex center	264	11	x	-	x	x	x	x

Table 4.3: Organic geochemistry: list of pore water, sediment and gas sampling sites where subsamples for shore-based analyses were obtained

Station	Site	Core length [cm]	Samples	CH_4-C_5H_{12} (GC-FID)	$\delta^{13}C$-CH_4-C_5H_{12} (GC-c-IRMS)	δD-CH_4 (GC-py-IRMS)	VFA conc. (HPLC-py-MS)	$\delta^{13}C$-VFA (HPLC-py-MS)	Biomarkers (GC-MS)	$\delta^{13}C$-Biomarkers (GC-MS)
GC2	Reference	526	21	x	x	x	x	x	x	x
GC5	Giza center	296	12	x	x	x	x	x	x	x
GC7	Giza NW	340	11	x	x	x	x	x	x	x
MUC27	Giza center	34	10	x	x	x	x	x	x	x
MUC28	Reference	29	8	x	x	x	x	x	x	x
GC29	Giza center	121	3	x	x	x	x	x	x	x
GC30	Giza SW	492	8	x	x	x	x	x	x	x
GC32	Giza center/NW	268	10	x	x	x	x	x	x	x
GC34	Giza center/NW 2	420	16	x	x	x	x	x	x	x
GC36	North Alex center	271	22	x	x	x	x	x	x	x
GC38	North Alex NW	263	17	x	x	x	x	x	x	x
GC46	North Alex SE	276	12	x	x	x	x	x	x	x
MUC69	North Alex center	27	10	x	x	x	-	-	x	x
MUC70	North Alex NW	19	5	x	x	x	-	-	x	x
MUC71	North Alex center	31	12	-	-	-	x	x	-	-
GC74	North Alex center	294	-	-	-	-	-	-	-	-
GC100	North Alex center	264	11	x	x	x	x	x	x	x

4.4 Preliminary results

4.4.1 Giza MV

The pore water profiles of Cl-, TA, NH_4^+ and H_2S of Giza MV sediments are given in Fig 4.3. The Cl^- concentration decreases from a typical mediterranean bottom water value of 605 mM to about 140 mM at the lower end of the GCs. Such asymptotic pore water gradients are due to mixing of a deep fluid with bottom water. Cl^- depletion in MV fluids is usually assigned to mineral dehydration reactions (e.g. smecite to illite transformation) occurring at up to several km depth in the sedimentary stack beneath the mud volcano (e.g. Dählmann and de Lange, 2003). The respective depth where the transition from bottom water to deep fluid occurs, increases with increasing distance from the MV center (GC32, 280 cmbsf > GC34, 200 cmbsf, > GC5, 180 cmbsf). Thus, the site of most intense fluid advection of Giza MV is indeed located at or at least close to the geographical center. The Cl^- profile of GC29 shows a negative spike close to the surface and constant concentrations equal to Mediterranean bottom water below. The same peak is present in the TA and in the NH_4^+ profile. The lowermost Cl^- concentrations of the surface spike (140 mM) are equal to those of the deep fluid described above. Thus, it can be assumed that a recent mud flow, carrying the Cl^- pore water signal of the deep fluid, has covered the original sediment surface and disappears now successively due to molecular diffusion across the initial sediment surface and the benthic sediment/water interface.

The TA increases in most of the GCs to reach maximum values of about 130 meq L^{-1} at the lower core end. The downcore increasing alkalinity is most likely related to oxidation of advecting methane or other hydrocarbons. The NH_4^+ concentrations do also increase with depth but the maximum values are more heterogeneous than those for Cl^- and TA. NH_4^+ serves as a nutrient in marine systems and is progressively released into pore water during organic matter diagenesis. Thus, high NH_4^+ concentrations in the encountered MV fluids may be assigned to intense organic matter diagenesis or catagenesis in the sedimentary sequence beneath the MV.

The anaerobic oxidation of methane (AOM) transported upwards in solution in mud volcano fluids is performed by microbial consortia involving methane-oxidizing Archaea (ANME) and sulphate-reducing bacteria (Boetius et al., 2000), and the overall reaction releases high amounts of HCO_3^- and H_2S (Reeburgh, 1983). The detection of an H_2S production peak at a depth of ≈30 cmbsf at the center (GC5 and MUC27), of a bigger peak ≈150 cmbsf (GC34) and at ≈250 cmbsf (GC32) NW of Giza MV constitutes a preliminary indication that Giza MV fluids are highly enriched in CH_4 (and perhaps higher molecular homologues) which is oxidized in the near subsurface sediments at this MV. Moreover, the AOM zone lies closer to the surface when the upward-directed advection flux of CH_4-enriched fluids is more intense. Thus the shallower location of the AOM zone in the center than NW of Giza MV provides another indication that the venting activity is highest at the center. In excellent agreement with Cl^-, TA, NH_4^+ pore water profiles, the depth of H_2S production peaks decreasing from center (GC5, MUC27) to NW (GC34<GC32), and is either absent (i.e. no CH_4 influx and AOM), or located at depths greater than GC and MUC lengths, at SW of Giza MV (GC30).

4.4.2 North Alex MV

The pore water profiles of Cl^-, TA, NH_4^+ and H_2S of North Alex MV sediments are given in Fig. 4.4. The transition of bottom water Cl^- concentrations to that of the deep fluid (180 mM) occurs mainly above 100 cmbsf at the center of North Alex MV, at shallower depth than at Giza MV. As a consequence, pore water dilution and H_2S production peak are fully developed in the first 22 cmbsf of MUC69 collected at the center of the mud volcano. Alkalinity and NH4+ concentrations increase with depth and reach maximum values of 100 meq L^{-1} and 2000 μM respectively, which is similar to the values obtained for GCs from Giza MV. Maximum

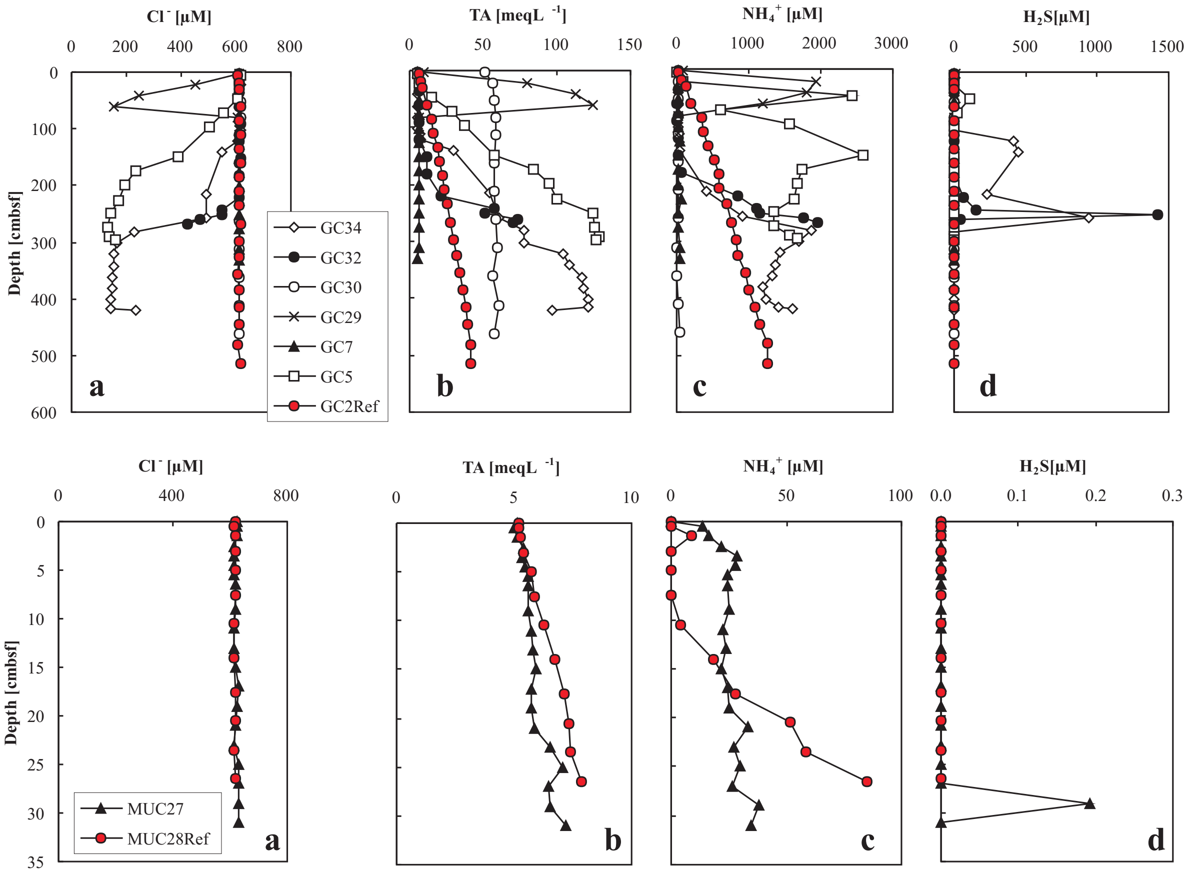

Figure 4.3: Pore water concentrations of (a) Cl^-, (b) TA, (c) NH_4^+ and (d) H_2S in gravity cores (upper row) and multi cores (lower row) from Giza MV. The reference cores are shown for comparison.

concentrations of dissolved sulfide are by one order of magnitude higher and occur at shallower depth compared to Giza MV. The pore water samples of GC36 and GC46 were yellowish which can perhaps be assigned to the very high sulfide or sulfur concentrations (up to 15500 μM). Also, elevated H_2S concentrations are observed over a broad depth range of 200 cm or more in cores GC46 and GC38. In core GC36 and MUC69 from the center, the H_2S production peak is more constrained and is probably associated with AOM sustained by intense upward-directed flux of CH_4-enriched fluids at this very active MV (see also temperature data in section 6). The H_2S concentration peak at the center of North Alex MV occurs within the first 5 to 15 cmbsf, closer to the seafloor than at the center of Giza MV, consistent with other geochemical and temperature indications for more intense venting activity at North Alex MV. Moreover, all North Alex MV sediments, but especially those of cores GC36 and GC46, are characterized by the presence of bivalves and authigenic precipitates such as carbonate chimneys (Fig. 5.3) and macroscopic euhedral pyrite crystals visible on the surface of nodule clasts (Fig. 5.4) whose formation is mediated by microorganisms thriving at cold and hydrothermal seeps (eg Hinrichs et al., 1999; Pancost et al., 2001).

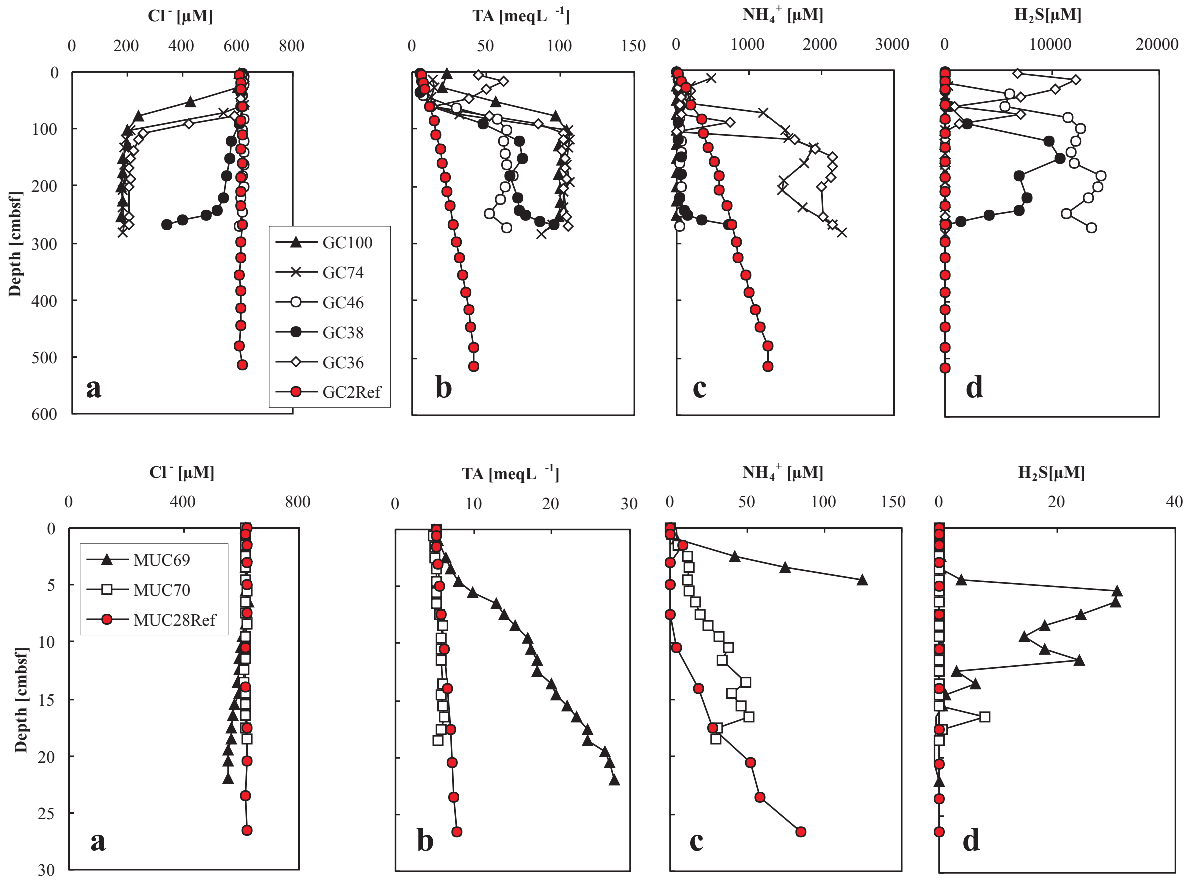

Figure 4.4: Pore water concentrations of (a) Cl^-, (b) TA, (c) NH_4^+ and (d) H_2S in gravity cores (upper row) and multi cores (lower row) from North Alex MV. The reference cores are shown for comparison.

Chapter 5

Sedimentology / Micropalaeontology

Kevin Brown and Janne Lorenzen

5.1 Introduction

The aims of the sedimentological and micropalaeontological research carried out during the P362/2 cruise was to study the sedimentary material being erupted from the North Alex and Giza mud volcanoes.

Mud volcanoes are believed to have a deep source of shale that has become fluidized and starts to move towards the surface. As it moves though the overlying strata small fragments of material are carried upwards. Studying these included fragments will give information about the underlying sedimentary structure below the mud volcanoes. Sampling of debris flow material down slope of the mud volcanoes for later studies into the activity of the two mud volcanoes was also carried out. Biostratigraphical dating of samples by use of included fossil foraminifera where present was also to be attempted.

5.2 Coring work

A total of 21 gravity cores (GC) and 5 Multicores (Muc) were taken during P362/2 (see Table 5.1). A total of 523 samples have been collected, 257 for geochemical analysis and 266 for sedimentology and micropalaeontology.

All cores were taken using a 6 m gravity core. The barrel was fitted with a hard PVC liner to facilitate removal of sediment core on recovery. On recovery the liner was cut into 1 m sections, capped and labelled. Cores were then split using a table saw, half the core being designated the work half, the other half the archive half.

All samples were taken form the work half, with the exception of a few large clasts, which were removed from the reference half to allow fitting into a "D-tube". On completion of sampling, any remaining sediment within the work half was put into a bucket mixed with water, then sieved through a 1 mm sieve to collect the remaining clasts from within the section.

The reference half first had its surface scraped to produce a smooth surface and clear film placed onto it. This was done to make identification of sedimentary structures easier. The sections were then examined to identify sedimentary structures, grain size, color and included clasts, the descriptions being recorded on preformatted sheets. On completion of the description the reference half was wrapped in clear film and placed in a D-tube, labelled and the end caps taped, the sections refrigerated for return to IFM-GEOMAR. Appendix A contains the complete core descriptions.

The multicorer was deployed a total of 5 times with varying degrees of success. Stations: 27 - 6 barrels, 28 - 7 barrels, 69 - 6 barrels, 70 - 5 barrels and 71 - 4 barrels. Multiple barrels were used for organic and inorganic geochemical sampling, and one barrel being used for sedimentology / micropalaeontological study. Five barrels are being returned to IFM-GEOMAR for microbiological studies.

To study the distribution of benthic foraminifera the protein stain Rose Bengal (2 g Bengal Rose in 1 lt of Ethanol) was used to distinguish between living and dead foraminifera, the stain colors protein bright pink. The core barrel was sampled at the following resolution: 0 - 0.5 cm, 0.5 - 1 cm, 1 - 2 cm, 2 - 3 cm, 3 - 4 cm and 4 - 5 cm. All samples were placed in large 500 ml pots and covered with twice the volume of Bengal Rose stain. Extra samples were taken further down each core barrel but these were not treated with ethanol. On completion of sampling the pots were labeled, taped and stored for return to IFM-GEOMAR.

Table 5.1: Gravity corer and multicorer stations. At North Alex MV, all positions were determined using the GAPS positioning system.

P362/2-	Device	Date	UTC	Site	Comment
2-2	GC	13/02/2008	16:35	Giza Reference	
5	GC	15/02/2008	11:23	Giza Center	
6	GC	15/02/2008	12:44	Giza Outflow	
7	GC	15/02/2008	14:00	Giza NW	
7-2	GC	15/02/2008	15:05	Giza NW	
27	MUC	16/02/2008	09:48	Giza Center	
28	MUC	16/02/2008	11:37	Giza Reference	
29	GC	16/02/2008	13:16	Giza Center	
30	GC	16/02/2008	14:25	Giza SW	
31	GC	16/02/2008	15:35	Giza NE	
32	GC	16/02/2008	16:41	Giza Center/NW	
33	GC	16/02/2008	17:56	Giza Reference	
34	GC	17/02/2008	06:48	Giza Center/NW	
36	GC	20/02/2008	04:45	N. Alex Center	GAPS
36-2	GC	20/02/2008	05:41	N. Alex Center	GAPS
37	GC	20/02/2008	06:45	N. Alex Outflow	GAPS
38	GC	20/02/2008	07:48	N. Alex NW	GAPS
46	GC	20/02/2008	16:36	N. Alex SE	GAPS
69	MUC	21/02/2008	07:59	N. Alex Center	GAPS
70	MUC	21/02/2008	09:44	N. Alex NW	GAPS
71	MUC	21/02/2008	11:07	N. Alex Center	GAPS
72	GC	21/02/2008	12:33	N. Alex Far Outfl.	GAPS
73	GC	21/02/2008	13:52	N. Alex Ref 3	GAPS
74	GC	21/02/2008	16:10	N. Alex	GAPS
99	GC	22/02/2008	06:26	N. Alex Ref 1	GAPS
100	GC	22/02/2008	07:31	N. Alex Center	GAPS

5.3 Preliminary results

5.3.1 Sedimentology

The dominant size fraction of the material recovered was fine silts and muds. When wet sieving at 62 μm 99% of material is lost through the sieve.

The cores taken on both mud volcanoes showed very little structure, having a distinctly different lithology when compared to the laminated sediments observed in the reference core (P362/2-2). Mud volcano sediments showed very little variation in color, dominantly Dark Gray to Very Dark Gray. Syringe samples of 10 ml volume were taken at various depths from all opened cores. These were labeled and stored for sedigraph studies of the finer size fraction (>62 μm) on return to IFM-GEOMAR.

Clasts can be broadly separated into two distinct types. Mudstones that show a similar color and lithology to the finer matrix but are greatly compacted (fig. 5.1); and fragments of rock that have completely different lithologies (fig. 5.2). The second group include sandstones (some quite coarse gained in partial size) and fragments of shales. The size of clasts ranges from >1 mm to several centimeters, color varies with rock type but they are distinct from the mud making collection of larger specimens easy. Large numbers of smaller clast specimens were obtained during washing down of core residue following sampling. These were dried, bagged, and labeled for further sorting and study on return to IFM-GEOMAR.

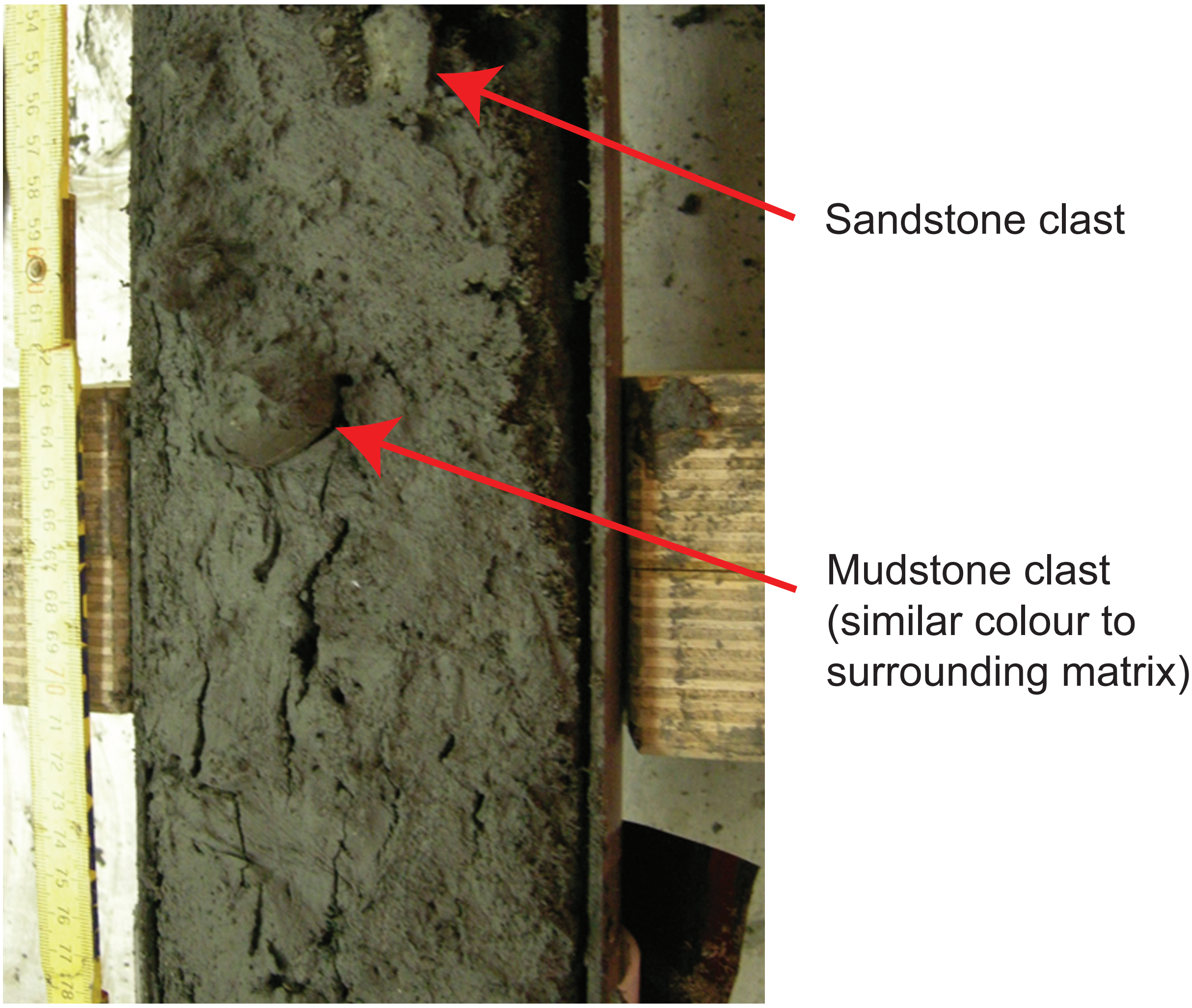

Figure 5.1: Example of large mudstone clast found in core P362/2-46, sec.1

Calcite micro chimneys and a large chimney (fig. 5.3) were found in core P362/2-38. The calcite was found in association with a large number of bivalve shells at a depth of approximately 75 cm below the top of the core. Many bivalve shells are firmly fixed within the chimney, which appears to have grown up around the shells. The presence of the bivalve shells indicates that this region was once much closer to the surface than at present. However it is not clear if the calcite chimney and the bivalve shells are of the same age, or the shells served as nucleation sites for the deposition of calcite at a later date. Figure 5.4 illustrates an apparent old chimney,

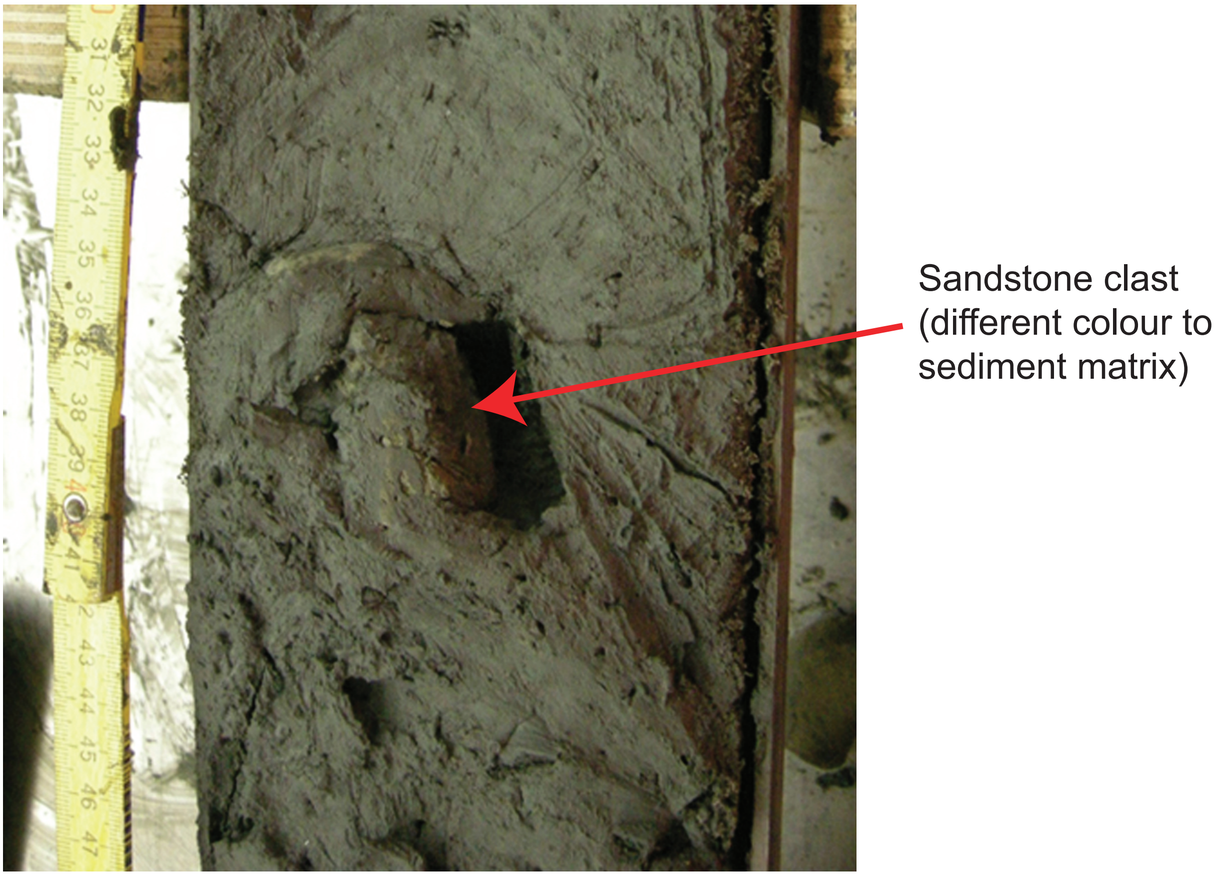

Figure 5.2: Example of large sandstone clast in core P362/2-46, sec.1

which is encrusted with pyrite and stained with iron. The surface is rough, which may indicate transport with in the muds of the volcano.

5.3.2 Micropalaeontology

Six core catcher samples and two surface samples were wet sieved at 62.5 μm and the residues studied under the binocular microscope.

No foraminifera were identified in the core catcher samples.

The surface samples came from P362/2-2 (Reference core) and liquid sediments from the top of P362/2-36 (North Alex center).

The hemipelagic sediments of P362/2-2 contained few planktonic foraminifera. Species identified were *Globigerinoides ruber*, *Globigerina bulloides*, and *Globorotalia truncatilinoides*. All three are contemporary species and endemic to the Eastern Mediterranean. Benthic foraminifera include specimens of *Cibicidoides sp. Bullomina inflata*, *Uvigerina mediterrania*, small *Brizalina* and *Bolovinia* species. It is particularly interesting because of the absence of agglutinated species. Repeat and further in depth studies are planned on core P362/2-2 on return to IFM-GEOMAR.

The sample from P362/2-36 contained no foraminifera. The material left following wet sieving was found to be small lithic fragments.

Further work on the clasts is planned to determine if they contain calcareous nanofossils, to assist in dating and identifying the source depth of the clasts below the mud volcano.

Figure 5.3: Close-up of carbonate chimney found in core P362/2-38-3. The chimney was situated approximately 75 cm below the surface. Bivalve shells are clearly visible and are firmly fixed to the chimney structure.

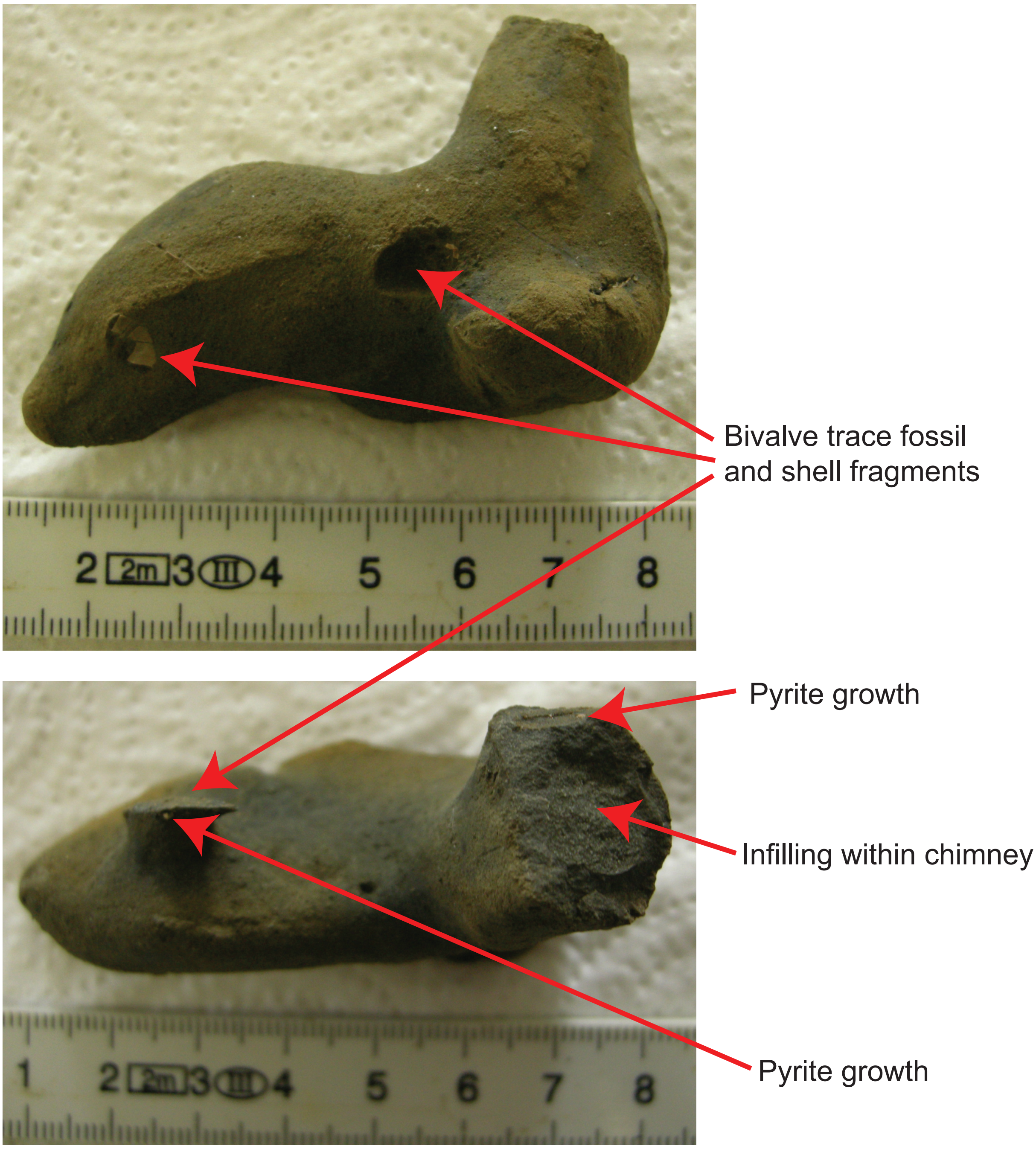

Figure 5.4: Old carbonate chimney found in core P362/2-100. Numerous small white dots are pyrite growths. Note apparent brown rust coloring.

Chapter 6

Heatflow and sediment temperature measurements

TOMAS FESEKER, WIEBKE NEHMIZ, AND GERO WETZEL

6.1 Introduction

The ascent of warm mud and water at mud volcanoes creates temperature anomalies close to the seafloor. In-situ sediment temperature and thermal conductivity measurements provide an excellent means to detect rapidly areas affected by seepage and form the basis of modeling studies to quantify transport processes at mud volcanoes (e.g. Feseker et al., 2008). Due to the time scales associated with the conduction of heat in marine sediments, repeated temperature measurements are also useful to describe temporal variability of seepage.

6.2 Materials and Methods

6.2.1 Heatflow probe

Characteristics

For this cruise, a heatflow probe in the so called violin bow design after Bullard (1954) was applied. This instrument was built by FIELAX GmbH, Bremerhaven. Operation on bord was taken care of by FIELAX GmbH. The active length of the probe is 5.67 m with 22 sensors for temperature measurements. Sensor spacing is 27 cm. The YSI-44032 thermistors measure temperature at a resolution of better than 1 mK and are calibrated to an accuracy of around 2 mK. Sensors for tilt, pressure, absolute water temperature and internal controls are implemented in addition to the temperature sensors.

For the determination of heatflow in the sediments, additional information on the thermal conductivity is necessary. The heatflow probe performs in situ conductivity measurements according to the pulsed needle probe method. A controlled amount of heat is introduced into the sediment, using an integrated heat wire. Observation of the temperature decay at all 22 sensors yields thermal conductivity of the surface layers at the sea floor.

Data recording was done into internal memory because no deep sea cable with a single conducting wire was available on *R/V Poseidon.* In automatic mode the energy supply and memory capacity is sufficient for nearly three days of continuous measurement.

The mechanical features of the heatflow probe are a length of 7.9 m and a weight of 1000 kg. Additional weight was available but not needed. All parts are rated to 600 bar or 6000 m of water depth. Temperature range for operation is from -2 °C to +60 °C. The construction is made of ultra-strong steel and can withstand an operation in gravel or even a drop on hard ground without being bent.

Operation

On *R/V Poseidon*, measurements were carried out using a trawl wire without the possibility of on-line data transfer. The deployment of the probe was done on the port side from the working deck. One crane was employed to heave the probe out of the trolley and horizontally over the side with a crow-foot. Another crane was employed for the rest of the station work with the trawl wire attached to the probe with a swivel. The process is illustrated in figure 6.1.

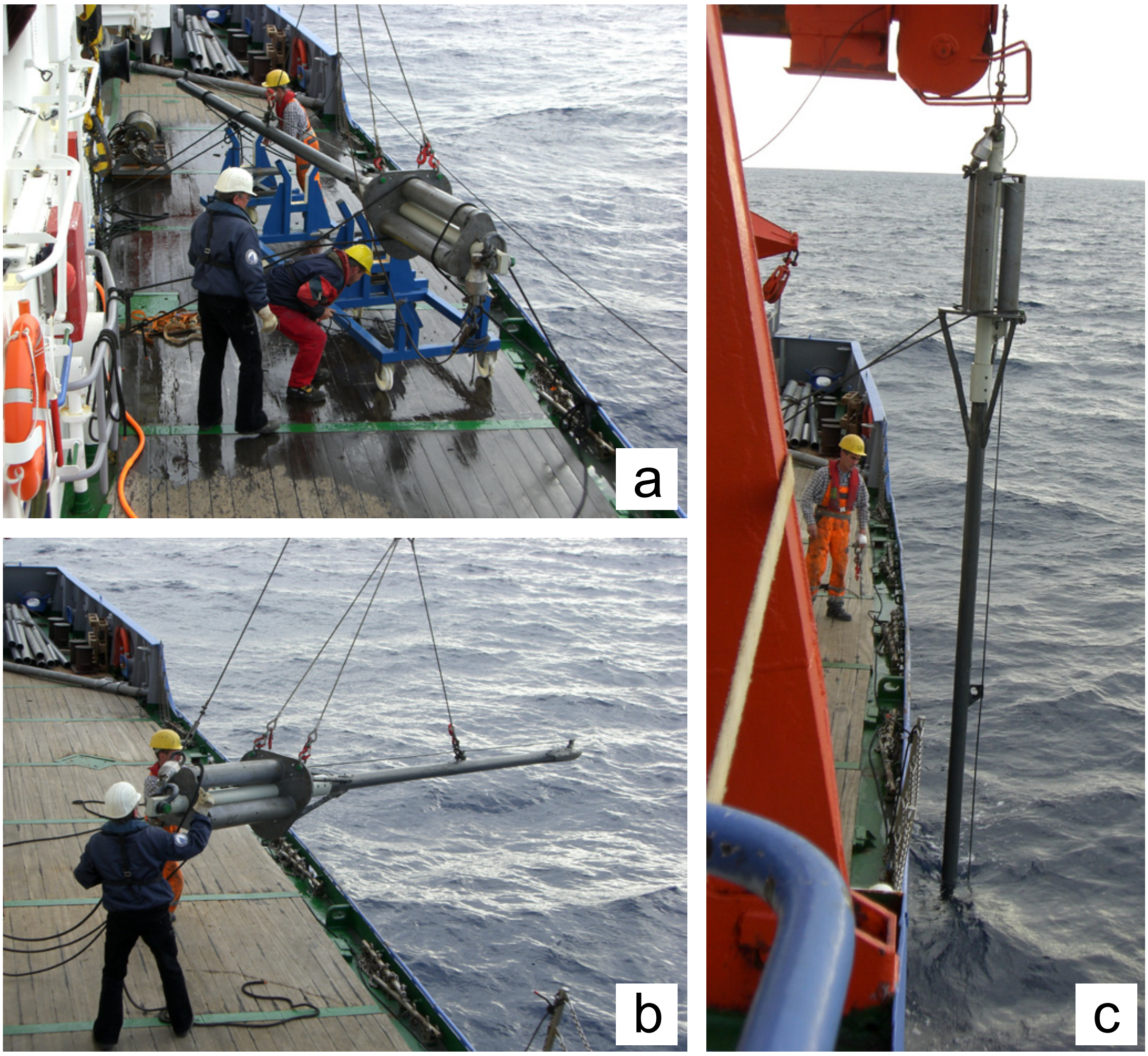

Figure 6.1: A trolley is used to transport the heatflow probe on the working deck (a). Using a crane, the instrument is heaved over the side in a horizontal position (b) and lowered vertically into the water (c).

A simple temperature measurement in the ground takes seven minutes after bottom contact. This time interval is needed for the frictional heat from penetration to decay and allow the sensors to adjust to the in-situ sediment temperatures. For measurements of in-situ thermal conductivity, a heat pulse is generated after this initial equilibration time, which makes it necessary that the probe remains in the sediment for another seven minutes to record the propagation of the heat pulse. The heat pulse is generated by heating the sensor string with a calibrated amount of energy. Afterwards, the decay of the temperature signal is measured. The heat pulse is triggered automatically with reference to time, tilt, pressure and their respective stabilities.

Operation during station work was controlled from the bridge, combining communication to both nautical staff and winch operators at close distance. Bottom contact was determined from a sharp decrease in cable tension. In the first working area at Giza MV, the ship's position at bottom contact was assumed to be the position of the probe at the sea floor. In the second working area at North Alex MV, a GAPS transponder was installed 50 m above the probe on the wire for a more accurate determination of the instrument at the seafloor.

Measurements with the heatflow probe were mainly done during the night, since no deck work is required during this time, only two crew members were needed for the winch. The deployment and recovery of the heatflow probe on *R/V Poseidon* needs at least five persons on deck. Consequently, deployment was done in the evening and recovery around breakfast time. Only part of transect 02 on North Alex (Station H0803) was done during daytime to ease the work for the geochemistry and the sedimentology group.

Two sensor strings and two electronic devices were used for the measurements during the cruise. Each sensor string was calibrated during the cruise to determine the relative temperature offsets of the individual sensors implemented in the string. During the calibration process, the heatflow probe is held in deep water for approximately 15 minutes without movement. These calibration measurements were done in the deepest regions of the two working areas to assure that the water temperature is constant over the length of the measuring interval.

Data conversion from temperature time series to temperature-depth data, called inversion, is performed using the program T2C, modified after an algorithm by Hartmann and Villinger (2002). This program allows the calculation of sediment temperatures after an infinite time of equilibration from limited time series and the determination of thermal conductivity values from a calibrated heat pulse.

6.2.2 In-situ sediment temperature measurements using the gravity corer

For integration of geochemical pore water data and in-situ temperature measurements into coupled transport models, it is important to know the thermal regime from which sediment samples are taken. This was accomplished by mounting three autonomous miniaturized temperature loggers (MTLs) and a tilt meter on outriggers attached to the barrel of the gravity corer (figure 6.2). The MTLs measure temperature at a resolution of around 0.6 mK and were calibrated to an accuracy of 2 mK before the cruise. Temperature measurements were conducted at all gravity corer stations during the cruise.

6.3 Work at sea

Station planning was along mostly SE-NW oriented transects to be able to steam against the wind and the current. These transects were planned to intersect in the center of the volcanoes, resulting in closely spaced stations in the central areas of the mud volcanoes, where the highest lateral temperature gradients were expected. On North Alex MV, weather conditions allowed two additional short transects across the central area in NE-SW direction.

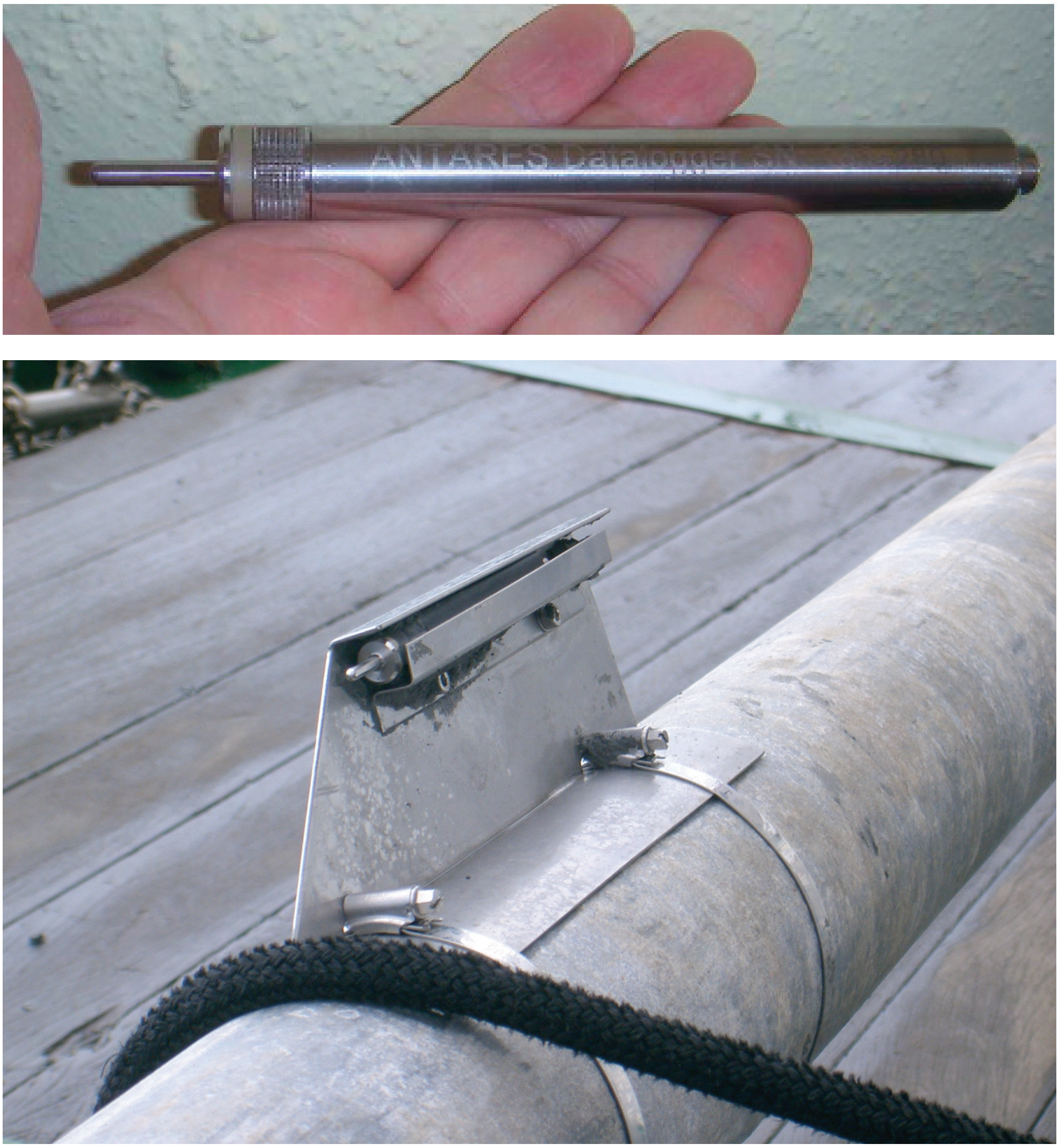

Figure 6.2: Miniaturized temperature loggers (MTLs) were mounted on outriggers attached to the barrel of the gravity corer to determine the thermal regime from which sediment samples were taken. The temperature sensor is located in the tip of the housing.

6.3.1 Giza MV

The heatflow probe was deployed at 20 stations on and around Giza MV, 19 of which yielded successful sediment temperature measurements. No data is available for station 23, because the tilt meter indicated that the heatflow probe had fallen over. Consequently, the measurements for this station were not processed. As shown in figure 6.3, the stations were located on two transect lines across the central area and at a reference site NE of the mud volcano.

Thermal conductivity measurements were conducted at stations 3, 8, and 19. However, only the data from the first two stations could be processed.

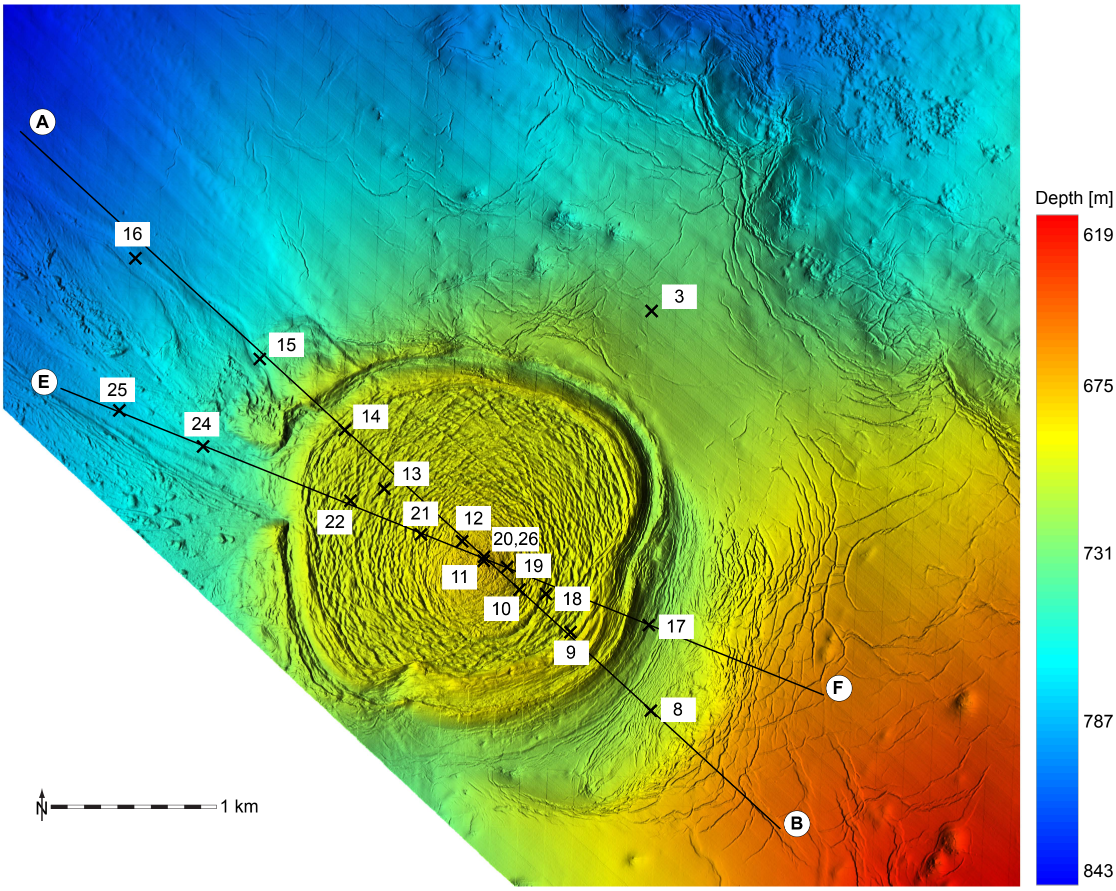

Figure 6.3: Heatflow probe stations at Giza MV. (DTM courtesy of BP)

6.3.2 North Alex MV

At North Alex MV, the heatflow probe was deployed at 53 stations. All deployments were successful except for station 42, where the tilt meter indicated that the heatflow probe had fallen over and the measurements could not be evaluated. As illustrated in figures 6.4 and 6.5, the alignment of the stations along transect lines across the central area resulted in a very high spatial resolution of the measurements in the central area.

Thermal conductivity measurements were conducted at 11 stations. However, the extremely high natural sediment temperatures in the central area rendered the generated heat pulse virtually ineffective, which resulted in 5 failed measurements.

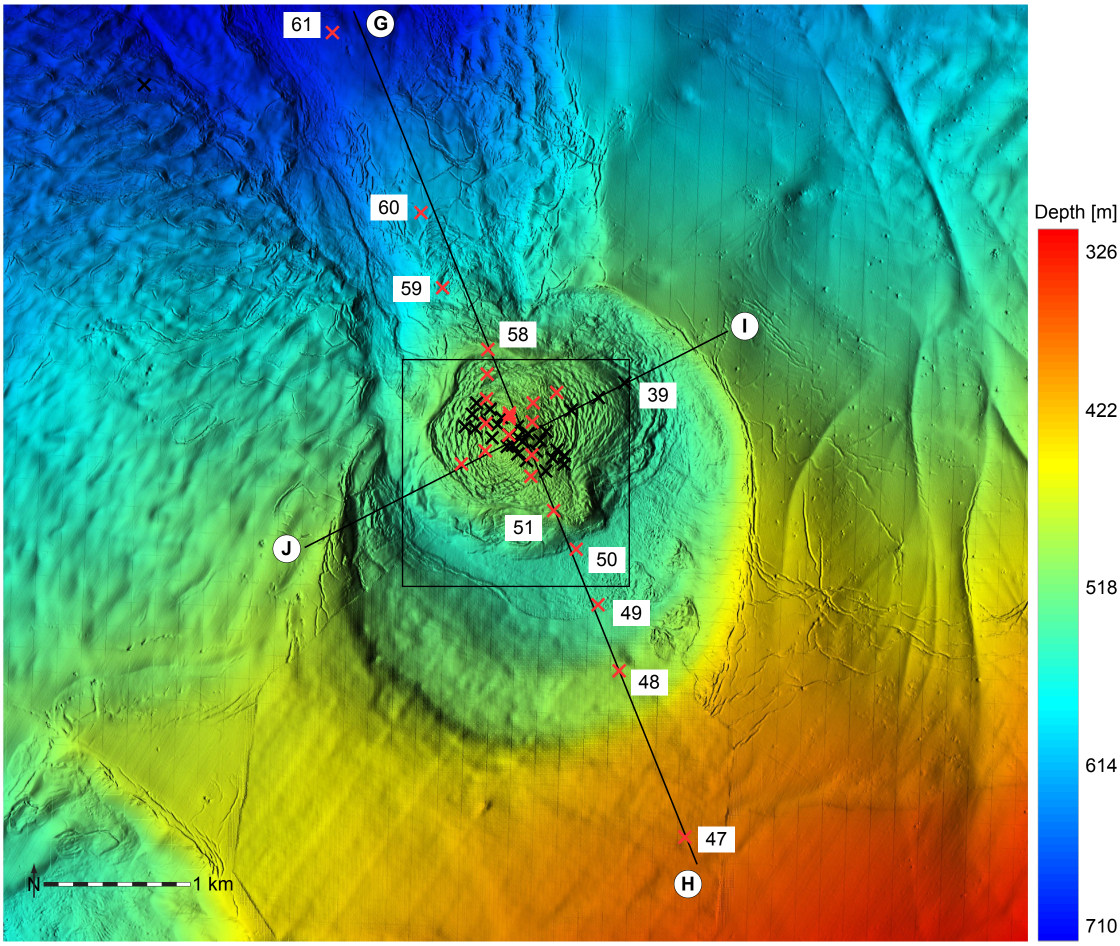

Figure 6.4: Heatflow probe stations at North Alex MV. GAPS positioning was used for all stations marked by black crosses. Red crosses indicate stations where the GAPS system was not working correctly and the position had to be determined less accurately using the ship's GPS receiver. The black rectangle shows the region of the enlarged map shown in figure 6.5. (DTM courtesy of BP)

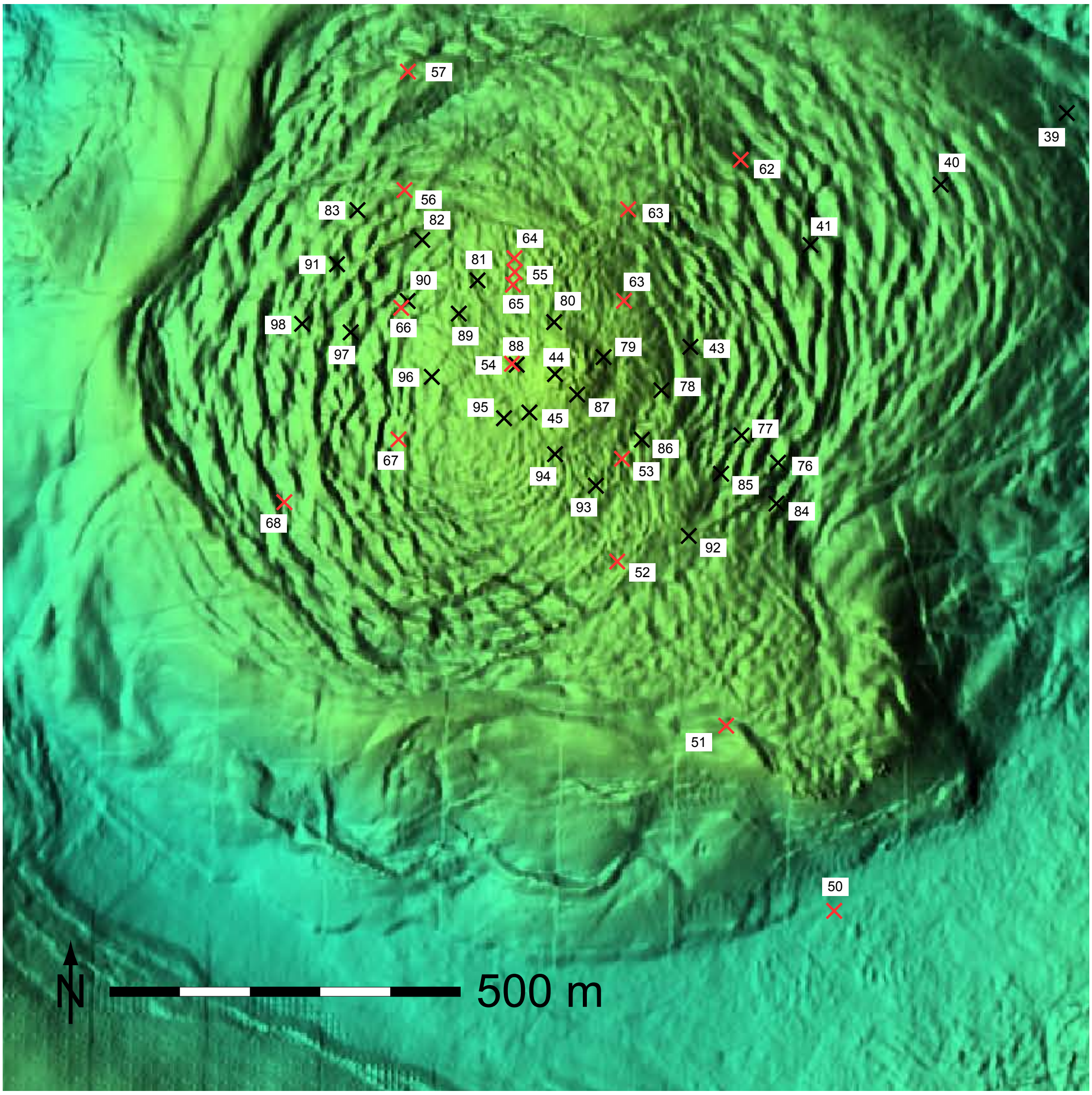

Figure 6.5: Heatflow probe stations in the central area of North Alex MV. GAPS positioning was used for all stations marked by black crosses. Red crosses indicate stations where the GAPS system was not working correctly and the position had to be determined less accurately using the ship's GPS receiver. The boundaries of this enlarged map is indicated by the black rectangle in figure 6.4. (DTM courtesy of BP)

6.4 Preliminary results

Preliminary results confirm that both Giza and North Alex MVs are currently active and indicate that seepage is focussed at the centers. At the time of observation, extremely high sediment temperatures at North Alex MV suggested higher seepage rates compared to Giza MV. In addition, the temperature distribution in the sediments was much more heterogeneous at North Alex MV, which points to a more transient thermal regime, possibly due to higher variability or recent mud expulsion.

6.4.1 Giza MV

In-situ sediment temperatures of around 40 °C at five meters below the seabed suggest a high level of activity at the center of Giza MV (figure 6.6). The temperature gradient decreases rapidly from more than 4 °C/m at the center to between 0.02 and 0.03 °C/m close to the edge, which corresponds to the regional background measured at the reference stations away from the mud volcano. Temperature profiles measured at 1800 and 2300 m WNW of the center showed multiple relative maxima that could be explained by the consecutive deposition of several large mud flows within the past decades as the temperature signature of the individual mud flows decays within a few years (figure 6.7).

The mean in-situ thermal conductivity at stations 03 and 08 was 0.86 and 0.87 $W/(mK)^{-1}$, respectively.

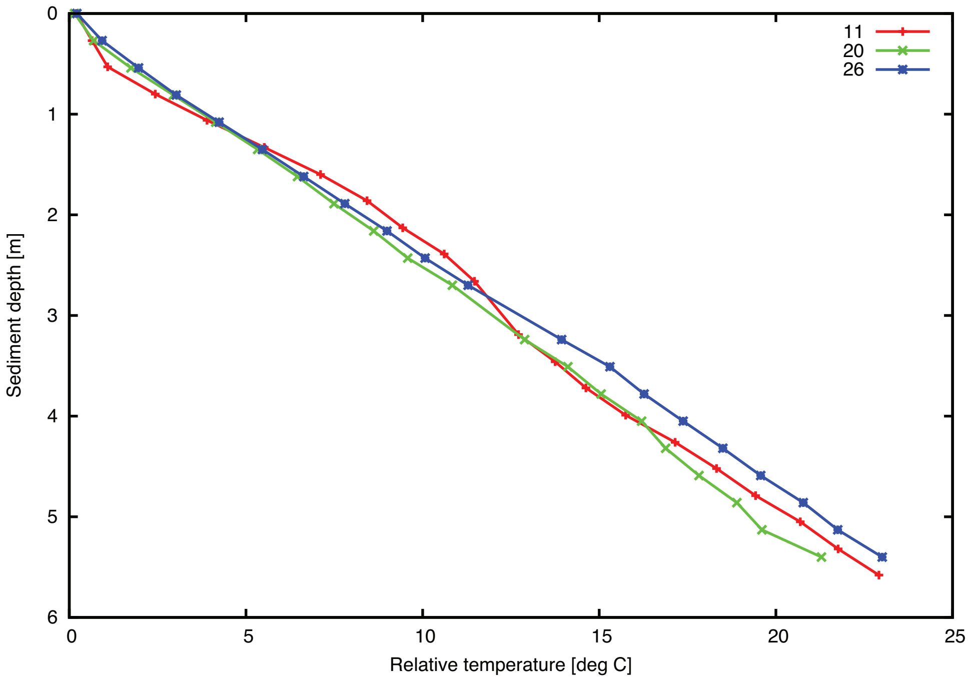

Figure 6.6: Relative temperature profiles with respect to bottom water temperature of around 13.8 °C from the center of Giza MV. The profiles measured during three deployments of the heatflow probe without the GAPS positioning system are in good agreement with each other, which suggests relatively low thermal heterogeneity at the center.

6.4.2 North Alex MV

In-situ temperatures reaching up to more than 70 °C at five meters below the seabed at the center of North Alex MV (figure 6.8) point to even higher rates of fluid flow than at Giza MV

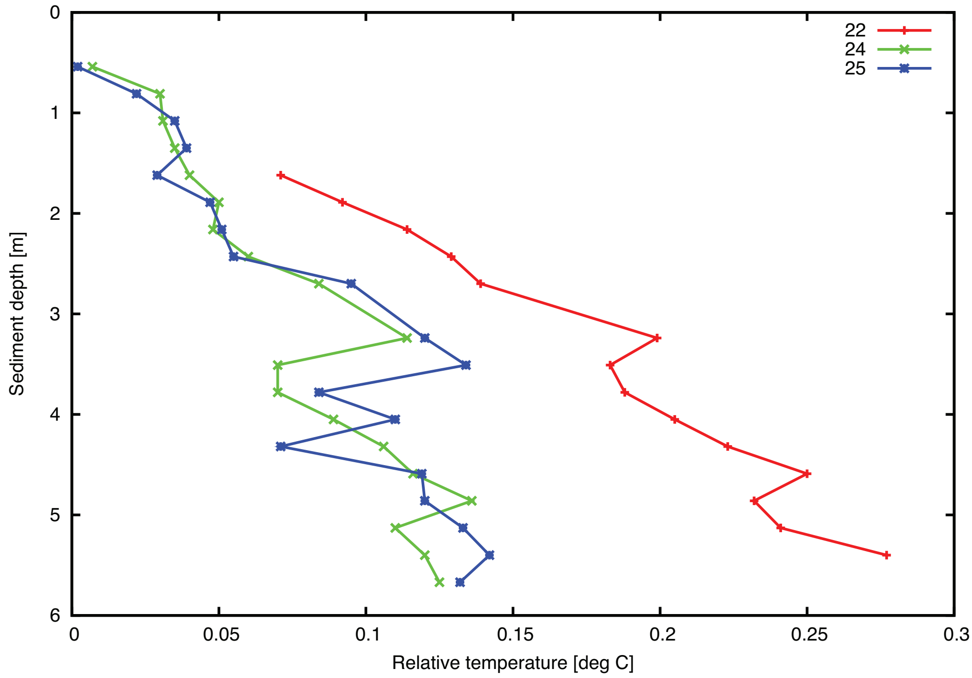

Figure 6.7: Relative temperature profiles with respect to bottom water temperature of around 13.8 °C. The relative maxima in profiles at distances of approximately 430 (22), 1800 (24), and 2300 m (25) WNW' from the center of Giza MV occur at roughly the same depths, which could be explained by the consecutive deposition of several mud flows.

and suggest very recent mud expulsion. The temperature gradient decreases from between 10 and 12 °C/m at the center to between 1 and 5 °C/m within a distance of less than 100 m, which is indicative of focussed seepage. Comparing the extremely high temperature gradient at the center to around 0.5 °C/m measured over the upper seven meters of the sediment column at the same location in 2003 (J.-P. Foucher, unpublished data) reveals the high temporal variability of mud volcano activity.

The mean in-situ thermal conductivity ranged between 0.89 and 1.03 $W/(mK)^{-1}$.

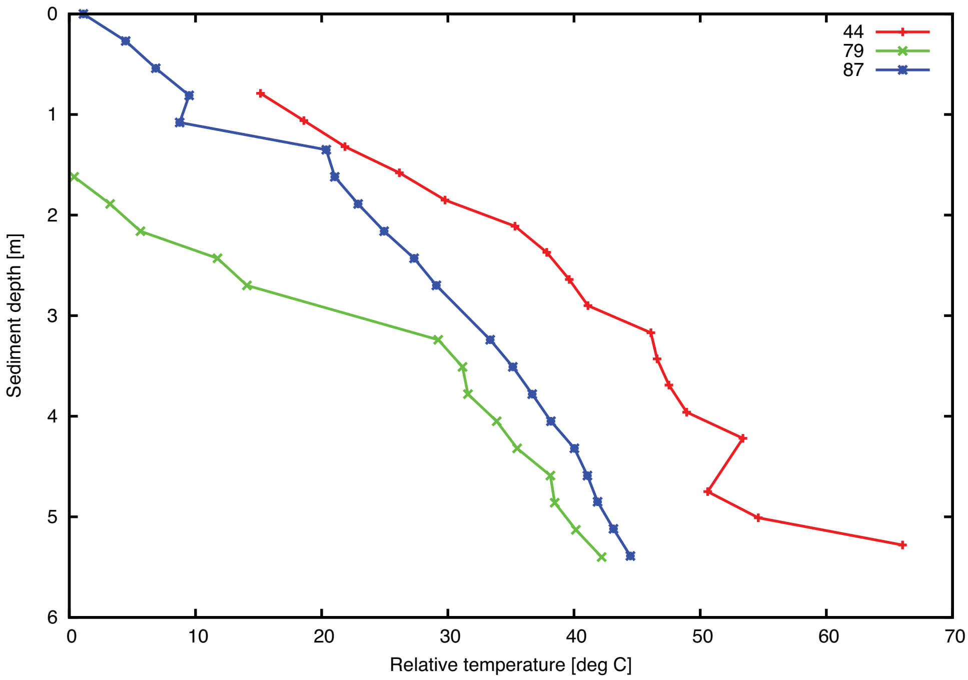

Figure 6.8: Relative temperature profiles with respect to bottom water temperature of around 13.8 °C from the center of North Alex MV. According to the GAPS positioning system used for all three deployments, the locations are distributed around the highest point of the central mud volcano, at distances between 40 and 75 m from each other. While part of the deviations between the profiles may be attributed to errors in the estimated penetration depth, the thermal heterogeneity is relatively high, suggesting a transient regime following a recent seepage or mud expulsion event.

References

Boetius, A., Ravenschlag, K., Schubert, C. J., Rickert, D., Widdel, F., Gieseke, A., Amann, R., Jorgensen, B. B., U, W., Pfannkuche, O., 2000. A marine microbial consortium apparently mediating anaerobic oxidation of methane. Nature 407, 623–626.

Bowes, H. L., Hornibrook, E. R. C., 2006. Emission of highly ^{13}C-depleted methane from an upland blanket mire. Geophysical Research Letters 33, L04401, doi:10.1029/2005GL025209.

Bullard, E. C., 1954. The flow of heat through the floor of the Atlantic Ocean. Proceedings of the Royal Society of London. Series A 222, 408–429.

Dählmann, A., de Lange, G. J., 2003. Fluid-sediment interactions at Eastern Mediterranean mud volcanoes: a stable isotope study from ODP Leg 160. Earth and Planetary Science Letters 212 (3-4), 377–391.

de Beer, D., Sauter, E., Niemann, H., Kaul, N., Foucher, J.-P., Witte, U., Schlüter, M., Boetius, A., 2006. In situ fluxes and zonation of microbial activity in surface sediments of the Håkon Mosby Mud Volcano. Limnology and Oceanography 52 (3), 1315–1331.

Dupre, S., Woodside, J., Foucher, J.-P., de Lange, G., Mascle, J., Boetius, A., Mastalerz, V., Stadnitskaia, A., Ondreas, H., Huguen, C., Harmegnies, F., Gontharet, S., Loncke, L., Deville, E., Niemann, H., Omoregie, E., Olu-Le Roy, K., Fiala-Medioni, A., Dahlmann, A., Caprais, J.-C., Prinzhofer, A., Sibuet, M., Pierre, C., Damste, J. S., 2007. Seafloor geological studies above active gas chimneys off Egypt (Central Nile Deep Sea Fan). Deep Sea Research Part I: Oceanographic Research Papers 54 (7), 1146–1172.

Feseker, T., Foucher, J. P., Harmegnies, F., 2008. Fluid flow or mud eruptions? Sediment temperature distributions on Håkon Mosby mud volcano, SW Barents Sea slope. Marine Geology 247 (3-4), 194–207.

Grasshoff, K., Ehrhardt, M., Kremling, K., 1999. Methods of Seawater Analysis. Wiley-VCH, Weinheim.

Hartmann, A., Villinger, H., 2002. Inversion of marine heat flow measurements by expansion of the temperature decay function. Geophysical Journal International 148, 628–636.

Hinrichs, K.-U., Hayes, J. M., Sylvia, S. P., Brewert, P. G., De Long, E. F., 1999. Methane-consuming archeabacteria in marine sediments. Nature 398 (802-804).

Kopf, A. J., 2002. Significance of mud volcanism. Reviews of Geophysics 40 (2).

Loncke, L., Gaullier, V., Mascle, J., Vendeville, B., 2002. Shallow structure of the Nile deep-sea fan: interactions between structural heritage and salt tectonics; consequences on sedimentary dispersal. In: CIESM (Ed.), Turbidite systems and deep-sea fans of the Mediterranean and the Black seas. CIESM Workshop Series. Vol. 17. Monaco.

Loncke, L., Gaullier, V., Mascle, J., Vendeville, B., Camera, L., 2006. The nile deep-sea fan: An example of interacting sedimentation, salt tectonics, and inherited subsalt paleotopographic features;. Marine and Petroleum Geology 23 (3), 297–315.

Loncke, L., Mascle, J., Party, F. S., 2004. Mud volcanoes, gas chimneys, pockmarks and mounds in the Nile deep-sea fan (eastern mediterranean): geophysical evidences. Marine and Petroleum Geology 21, 669–689.

Mascle, J., Zitter, T., Bellaiche, G., Droz, L., Gaullier, V., Loncke, L., Party, P. S., 2001. The Nile deep sea fan: preliminary results from a swath bathymetry survey. Marine and Petroleum Geology 18, 471–477.

Mastalerz, V., de Lange, G. J., Dahlmann, A., Feseker, T., 2007. Active venting at the Isis mud volcano, offshore Egypt: Origin and migration of hydrocarbons. Chemical Geology 246 (1-2), 87–106.

McAullife, C., 1971. GC determination of solutes by multiple phase equilibration. Journal of Chemical Technology 1, 46–50.

Niemann, H., Losekann, T., de Beer, D., Elvert, M., Nadalig, T., Knittel, K., Amann, R., Sauter, E. J., Schluter, M., Klages, M., Foucher, J. P., Boetius, A., 2006. Novel microbial communities of the haakon mosby mud volcano and their role as a methane sink. Nature 443 (7113), 854–858.

Pancost, R. D., Hopmans, E., Damste, J. S., the Medinaut Shipboard Scientific Party, 2001. Archeal lipids in Meditarranean Cold Seeps: Molecular proxies for anaerobic oxidation. Geochimica et Cosmochimica Acta 65, 1611–1627.

Reeburgh, W. S., 1983. Rates of biogeochemical processes in anoxic sediments. Annual Review of Earth and Planetary Sciences 11 (269-299).

Sauter, E. J., Muyakshin, S. I., Charlou, J.-L., Schluter, M., Boetius, A., Jerosch, K., Damm, E., Foucher, J.-P., Klages, M., 2006. Methane discharge from a deep-sea submarine mud volcano into the upper water column by gas hydrate-coated methane bubbles. Earth and Planetary Science Letters 243 (3-4), 354–365.

Wallmann, K., Drews, M., Aloisi, G., Bohrmann, G., 2006. Methane discharge into the Black Sea and the global ocean via fluid flow through submarine mud volcanoes. Earth and Planetary Science Letters 248 (1-2), 544–559.

Werne, J. P., Haese, R. R., Zitter, T., Aloisi, G., Bouloubassi, I., Heijs, S., Fiala-Medioni, A., Pancost, R. D., Sinninghe Damste, J. S., de Lange, G., 2004. Life at cold seeps: a synthesis of biogeochemical and ecological data from Kazan mud volcano, eastern Mediterranean sea. Chemical Geology 205 (3-4), 367–390.

Appendix A

Core descriptions

Kevin Brown and Janne Lorenzen

A.1 P362/2-2-2, GC, Giza reference site

No	Interval [cm]	Depth [cm]	Description
6	0-36	0-10	Partially filled
		11	fine grained silty material color 7.5YR 5/3
		19	color change 7.5YR 6/4
		28-31	darker band ?
			Anoxic or oxidation surface color 7.5YR 7/3
5	36-136		fine grained silt general color 7.5 YR 7/3
		36-43	Burrow
		43-50	oxidation mottling, color 2.5Y 5/1 light brownish grey
		50-60	oxidation - darker patch at 59 cm fine grained sands
			including shell fragments
		70	Patch light brownish grey
		82-88	laminar banding / Patches
			Light bands 2.5Y 5/2 - grayish brown
			darker bands 2.5 Y 4/1 - dark gray
		90	clasts
		98	large sandstone clast ca. 3 x 1 cm
4	136-236		Fine grained silty material
			Continuous sequence of laminar banding
			all the way down section
			bands approx. 2 - 3 mm
			light bands - pale yellow 2.5 Y 8/2
			dark bands - dark gray 2.5 Y 4/1
		170-172	thick dark layer Very dark grayish brown - 2.5 Y 3/2
		186	black organic matter
		226	thick dark layer
3	236-326		Fine grained silty material
			Continuous sequence of laminar bands.
			All bands perpendicular to liner
			light bands - pale yellow 2.5 Y 8/2
			dark bands - dark gray 2.5 Y 4/1
		302	Sandy coarser grained band containing shell fragments

No	Interval [cm]	Depth [cm]	Description
2	336-436		
		386	light band of courser material hard layer
			all the way across core
			color - Light yellowish brown 2.5Y6/3
			change in thickness of laminar bands. 4 - 6 mm
		429	Compacted silty material
			- light yellow brown color 2.5Y6/3
1	436-536		Fine grained silts
			laminar banding down length of section
			Light bands - Pale yellow - 2.5Y8/2
			Dark bands - Very dark grayish brown - 2.5Y3/2
			void at base of core due to core catcher

A.2 P362/2- 5, GC, Giza center

No	Interval [cm]	Depth [cm]	Description
4	0-10		Very liquid surface sediment
			no color description
			sampled in a plastic bag
3	10-110		Homogenous no structure
			Overall color Very dark gray - 2.5Y3/1
			scattered mud clasts color Grayish brown - 2.5Y5/2
		70-75	void
2	110-210		Homogenous no structure
			Overall color Very dark gray - 2.5Y3/1
			scattered mud clasts color Grayish brown - 2.5Y5/2
		110-148	Void
1	210-310		Homogenous no structure
			Overall color Very dark gray - 2.5Y3/1
			scattered mud clasts color Grayish brown - 2.5Y5/2
			void at the bottom due to core catcher

A.3 P362/2- 6, GC, Giza Outflow

No	Interval [cm]	Depth [cm]	Description
5	0-15		
4	15-115		
3	115-215		
2	215-315		
1	315-415		

Core cut into sections and stored, no work carried out onboard. All lengths are estimates based on measurements of the outside of the liner.

A.4 P362/2- 7, GC, Giza NW

No	Interval [cm]	Depth [cm]	Description
4	0-91		Very fine grained sediments
			? Pelagic in origin
		0-4	color Dark Gray - 7.5YR4/1
		4-7	band dark brown - 7.5YR4/4
			Mottling in sediments
			- color changes not sedimentary structures
		21-28	Gray band - 2.5Y5/1
		28-40	mixed patches of Dark gray and dark brown coloring
		40-64	Dark Grey colored sediment (2.5Y4/1)
			no structure visible
		62	shell band
		62-9	mixed patches of Dark gray and Gray
3	91-191		Homogenous no recognized bedding structures
			mottled sediments with scattered lighter clasts
			General color Very dark grey - 2.5Y3/1
		110-112	shale fragments approx. 3 - 4 mm dia.
2	191-291		Homogenous no structure
			General color Dark grey - 2.5Y4/1
			Scattered clast thought out section
			size varies between 1-5 mm dia.
			Light color clasts - Light yellowish brown 2.5Y6/3
			Dark clasts ? Mudstones color Gray 2.5Y5/1
		205-235	Light olive brown (2.5Y5/6)
			staining on left side of core approx 1.5cm wide
1	291-340		Homogeneous no structure
			General color Dark grey - 2.5Y4/1
			Scattered clast thought out section
			size varies between 1-5 mm dia.
			Light color clasts - Light yellowish brown 2.5Y6/3
			Dark clasts ? Mudstones - color Gray 2.5Y5/1

A.5 P362/2- 7-2, GC, Giza NW

Core cut into 4 sections and stored, no work carried out onboard. Estimated total length of core is 330 cm.

A.6 P362/2- 29, GC, Giza Center

No	Interval [cm]	Depth [cm]	Description
2	0-80		Homogenous no structure visible
			scatter clasts towards bottom of section
			General color - Very dark Gray 10YR3/1
			clast color Grayish brown 10YR5/2
1	80-120		Homogenous no structure visible
			scattered clasts
			General color - Very dark Gray 10YR4/1
			clasts color Grayish brown 10YR5/2
		82-86	dark smear Very dark gray 2.5Y3/1
		93-96	smear of light grey 2.5Y5/1
			void due to core catcher at base of core.

A.7 P362/2- 30, GC, Giza SW

No	Interval [cm]	Depth [cm]	Description
6	0-26		very soft ? Pelagic sediments
			Oxic
			color Dark Yellowish brown 10YR4/4
			with lighter yellowish brown (10YR5/6) stripes
5	26-126		Fine grained silts not visible structures
			? Pelagic sediments.
		29-50	gradual color change
			from brown (10YR5/3) to Gray 2.5Y5/1
			no visible clasts
		118	small dark smears (Grey 2.5Y5/1)
4	126-227		No structure
			color mottling:
			2.5Y5/1 - Gray
			2.5Y4/1 - Dark Gray
			no clasts
		144-178	brown (10YR5/3) stain on right side of core
3	227-327		No structure no clasts, colored spots.
			mottling color change between Gray and dark Gray
2	327-427		No sedimentary structures. colored bands visible
			General color Gray to Dark Gray (2.5Y5/1 to 2.5Y4/1)
			calcite (pale yellow 2.5Y7/3) at:
		351	fragments
		364	? Calcite hard layer
		392	Calcite fragments
		401	calcite
1	427-489		No structure visible, no clasts
			colored Mottling
			gray and dark gray
			lighter spots (pale yellow 2.5Y7/3)

A.8 P362/2- 31, GC, Giza NE

Core cut into 4 sections and stored, no work carried out onboard. Estimated total length of core is 330 cm.

A.9 P362/2- 32, GC, Giza Center/NW

No	Interval [cm]	Depth [cm]	Description
3	4-104		Top of core very liquid collected in a bag
			oxic surface - Dark grayish brown 10YR3/2
			no visible structure color changes
			General color Dark Gray - 2.5Y4/1
		35-50	color banding, no visible difference in
			sedimentary structure
			color dark grayish brown (2.5Y4/2)
		68-104	small clasts ? Clay stone color light gray 2.5Y7/2
2	104-205		homogenous no structure no bedding...
			back ground color dark gray
			scattered clasts size 2 - 5 mm
			black clasts (2.5Y2.5/1)
			light soft clay stone clasts light gray 2.5Y7/2
			mottling towards of section.
1	205-267		no structures visible
			background color 2.5Y4/1
		205-247	color varies between black and Gray
		247-255	very liquid layer very strong Hydrogen sulphide smell
		255-267	very firm layer

A.10 P362/2- 33, GC, Giza Reference

Core cut into 6 sections and stored, no work carried out onboard. Estimated total length of core is 575 cm.

A.11 P362/2- 34, GC, Giza Center - Center/NW

No	Interval [cm]	Depth [cm]	Description
5	0-59		Very soft surface olive brown (2.5Y4/2) in color
			no observable structures
			very fine grained silts
			overall color dark gray (2.5Y4/1)
		42-43	large clasts
4	59-159		Fine grained silts and muds not visible structure
			scattered clasts
		103	clasts 4mm dia
		106	clasts 6mm dia
		120-129	large clast
		139	small clast pale yellow in color
3	159-259		1 m core section with small
			piece of sediment in 208 - 219 cm
			dark gray in color, dry appearance but
			sticky to touch...
2	259-359		Dry Clay "blocky" texture breaks easily into lumps
			Dark gray color (2.5Y4/1)
			sticky to touch - low water content.
		294-298	large clay stone clast, harder than matrix
			but same color
		317	color change - black (2.5Y2.5/1)
		334	dark clast (dark gray color 2.5Y4/1)
		349	5mm grayish brown clast (10YR5/2)
1	360-421		Overall Clay
			Dark gray color (2.5Y4/1)
		366	dark clast (dark gray color 2.5Y4/1)
		387-390	dark clast (dark gray color 2.5Y4/1)
			appears to be of similar material
			to matrix but more compacted
			void due to Core catcher at base of core.

A.12 P362/2- 36, GC, North Alex Center

No	Interval [cm]	Depth [cm]	Description
3	10-110		Top 10cm very liquid in a plastic bag.
			homogenous no visible structure
			strong hydrogen sulphide smell
			fine grained mud
			color very dark gray 2.5Y3/1
2	110-173		fine grained muds
			color very dark gray 2.5Y3/1
		113-115	large clast
		128-132	dry patch
		139-143	void
		154	clast
1	173-234		homogenous no sedimentary structure visible
			General color very dark grey (2.5Y3/1)
		177-180	band of lighter color small clasts
			color light gray (2.5Y7/2)
		192-198	compacted mud stone, appears to be
			of same material as matrix
			scattered small clasts

A.13 P362/2- 37, GC, North Alex Outflow

No	Interval [cm]	Depth [cm]	Description
5	0-60		
4	60-160		
3	160-260		
2	260-360		
1	360-400		

Core cut into sections and stored, no work carried out onboard. All lengths are estimates based on measurements of the outside of the liner.

A.14 P362/2- 38, GC, North Alex NW

No	Interval [cm]	Depth [cm]	Description
3	5-105		Top 5 cm very liquid collected in a plastic bag.
			Homogenous, no structure
			strong Hydrogen sulphide smell
			bubble structure visible in sediment
			General color Dark Grey 2.5Y4/1
		26	band of calcite fragments
		26-95	large numbers of calcite fragments ? Autogenic in origin
			mixed with shells
		76-82	Calcite chimney removed
2	105-205		homogenous no structure bubble structure to sediment
			strong Hydrogen sulphide smell
			General color Very Dark Grey 2.5Y3/1
		105-107	void
		179-181	large clast
		189-190	very large clast removed
		197-201	very large clast removed
1	205-266		homogenous no structure
			strong Hydrogen sulphide smell
			General color Vry Dark Grey 2.5Y3/1
			scattered clasts

A.15 P362/2- 46, GC, North Alex SE

No	Interval [cm]	Depth [cm]	Description
3	15-116		Top 5cm very liquid in plastic bag. homogenous muds no visible structure abundant small clasts strong Hydrogen sulphide smell mottling of colors top of the section is darker varies between black at top to very dark grey at bottom
2	116-218		Homogeneous no structure clasts found throughout core range in size from 2mm to 8 mm dia. many are compacted mudstones that appear to of the same material of the matrix but more compacted.
1	218-278		Homogenous no visible structure. strong Hydrogen sulphide smell very fine grained muds small clasts found all over the section General color Dark Gray - 2.5Y3/1
		260	clay stone clasts light olive brown (2.5Y 5/3) - 13mm dia
		278	clay stone clasts light olive brown (2.5Y 5/3) - 9mm dia

A.16 P362/2- 72, GC, North Alex Far Outflow

No	Interval [cm]	Depth [cm]	Description
6	0-55		
5	55-155		
4	155-255		
3	255-355		
2	355-455		
1	455-555		

Core cut into sections and stored, no work carried out onboard. All lengths are estimates based on measurements of the outside of the liner.

A.17 P362/2- 73, GC, North Alex Reference 3

No	Interval [cm]	Depth [cm]	Description
6	0-75		
5	75-175		
4	175-275		
3	275-375		
2	375-475		
1	475-533		

Core cut into sections and stored, no work carried out onboard. All lengths are estimates based on measurements of the outside of the liner.

A.18 P362/2- 74, GC, North Alex Center

This core was taken using a pre-drilled liner for pore water sampling with rhizons. Total length of the core was 294 cm. All of the core was used for sampling.

A.19 P362/2- 99, GC, North Alex Reference 1

No	Interval [cm]	Depth [cm]	Description
6	0-58		
5	58-158		
4	158-258		
3	258-358		
2	358-458		
1	458-523		

Core cut into sections and stored, no work carried out onboard. All lengths are estimates based on measurements of the outside of the liner.

A.20 P362/2- 100, GC, North Alex Center

No	Interval [cm]	Depth [cm]	Description
3	0-70		General
			Very fine grained silts and muds
			Faint Hydrogen sulphide smell
			color Dark Gray (2.5Y4/1)
			Abundant small clasts scattered throughout section
			Very liquid at top becomes firmer around 45 cm
		58-64	cavity left by large clast.
2	70-170		Very fine grained silts and muds
			General color Very Dark Gray 2.5Y3/1
		100-103	large clay stone clasts Dark Gray 2.5Y4/1 - removed
		107-113	large clay stone clasts Dark Gray 2.5Y4/1 - removed
		140-144	Dry blocky structure, small cavities ? Gas bubbles
		160-165	depression due to clay stone.
1	170-265		Very fine grained silts and muds
			General color Very Dark Gray 2.5Y3/1
		207-208	Clay stone clast light yellow brown 2.5Y6/4
		219-226	Partially filled section of core liner
		226-265	abundant scattered small clasts - Dark Gray 2.5Y3/1
			void a base of section due to core catcher.

Appendix B

Cruise Participants

Chief scientist		
Dr. Tomas Feseker	IFM-GEOMAR Wischhofstr. 1-3 D-24148 Kiel Germany	tfeseker@ifm-geomar.de

Observer		
Lt Cdr Ahmed Kamal Naguib	Egyptian Navy Hydrographic Office Alexandria Egypt	ahmedkamal76@hotmail.com

Geochemistry		
Dr. Marianne Nuzzo	IFM-GEOMAR	mnuzzo@ifm-geomar.de
Florian Scholz	IFM-GEOMAR	fscholz@ifm-geomar.de
Anke Bleyer	IFM-GEOMAR	ableyer@ifm-geomar.de
Regina Surberg	IFM-GEOMAR	rsurberg@ifm-geomar.de

Sedimentology/Micropaleontology		
Dr. Kevin Brown	IFM-GEOMAR	kbrown@ifm-geomar.de
Janne Lorenzen	IFM-GEOMAR	jannelorenzen@web.de

Sediment temperature measurements		
Wiebke Nehmiz	FIELAX GmbH Schifferstr. 10-14 D-27568 Bremerhaven Germany	nehmiz@fielax.de
Gero Wetzel	FIELAX GmbH	wetzel@fielax.de

Gravity- and Multicoring		
Thorsten Schott	OKTOPUS GmbH Wischhofstr. 1-3 D-24148 Kiel Germany	tschott@ifm-geomar.de

IFM-GEOMAR
Leibniz-Institut für Meereswissenschaften
an der Universität Kiel

IFM-GEOMAR Reports

No.	Title
1	RV Sonne Fahrtbericht / Cruise Report SO 176 & 179 MERAMEX I & II (Merapi Amphibious Experiment) 18.05.-01.06.04 & 16.09.-07.10.04. Ed. by Heidrun Kopp & Ernst R. Flueh, 2004, 206 pp. In English
2	RV Sonne Fahrtbericht / Cruise Report SO 181 TIPTEQ (from The Incoming Plate to mega Thrust EarthQuakes) 06.12.2004.-26.02.2005. Ed. by Ernst R. Flueh & Ingo Grevemeyer, 2005, 533 pp. In English
3	RV Poseidon Fahrtbericht / Cruise Report POS 316 Carbonate Mounds and Aphotic Corals in the NE-Atlantic 03.08.–17.08.2004. Ed. by Olaf Pfannkuche & Christine Utecht, 2005, 64 pp. In English
4	RV Sonne Fahrtbericht / Cruise Report SO 177 - (Sino-German Cooperative Project, South China Sea: Distribution, Formation and Effect of Methane & Gas Hydrate on the Environment) 02.06.-20.07.2004. Ed. by Erwin Suess, Yongyang Huang, Nengyou Wu, Xiqiu Han & Xin Su, 2005, 154 pp. In English and Chinese
5	RV Sonne Fahrtbericht / Cruise Report SO 186 – GITEWS (German Indonesian Tsunami Early Warning System 28.10.-13.1.2005 & 15.11.-28.11.2005 & 07.01.-20.01.2006. Ed. by Ernst R. Flueh, Tilo Schoene & Wilhelm Weinrebe, 2006, 169 pp. In English
6	RV Sonne Fahrtbericht / Cruise Report SO 186 -3 – SeaCause II, 26.02.-16.03.2006. Ed. by Heidrun Kopp & Ernst R. Flueh, 2006, 174 pp. In English
7	RV Meteor, Fahrtbericht / Cruise Report M67/1 CHILE-MARGIN-SURVEY 20.02.-13.03.2006. Ed. by Wilhelm Weinrebe und Silke Schenk, 2006, 112 pp. In English
8	RV Sonne Fahrtbericht / Cruise Report SO 190 - SINDBAD (Seismic and Geoacoustic Investigations Along The Sunda-Banda Arc Transition) 10.11.2006 - 24.12.2006. Ed. by Heidrun Kopp & Ernst R. Flueh, 2006, 193 pp. In English
9	RV Sonne Fahrtbericht / Cruise Report SO 191 - New Vents "Puaretanga Hou" 11.01. - 23.03.2007. Ed. by Jörg Bialas, Jens Greinert, Peter Linke, Olaf Pfannkuche, 2007, 190 pp. In English

10 FS ALKOR Fahrtbericht / Cruise Report AL 275 - Geobiological investigations and sampling of aphotic coral reef ecosystems in the NE-Skagerrak, 24.03. - 30.03.2006, Andres Rüggeberg & Armin Form, 39 pp.
In English

11 FS Sonne / Fahrtbericht / Cruise Report SO 192-1: MANGO: Marine Geoscientific Investigations on the Input and Output of the Kermadec Subduction Zone, 24.03. - 22.04.2007, Ernst Flüh & Heidrun Kopp, 127 pp.
In English

12 FS Maria S. Merian / Fahrtbericht / Cruise Report MSM 04-2: Seismic Wide-Angle Profiles, Fort-de-France – Fort-de-France, 03.01. - 19.01.2007, Ernst Flüh, 45 pp.
In English

13 FS Sonne / Fahrtbericht / Cruise Report SO 193: MANIHIKI Temporal, Spatial, and Tectonic Evolution of Oceanic Plateaus, Suva/Fiji – Apia/Samoa 19.05. - 30.06.2007, Reinhard Werner and Folkmar Hauff, 201 pp.
In English

14 FS Sonne / Fahrtbericht / Cruise Report SO195: TOTAL TOnga Thrust earthquake Asperity at Louisville Ridge, Suva/Fiji – Suva/Fiji 07.01. - 16.02.2008, Ingo Grevemeyer & Ernst R. Flüh, xx pp.
In English

IFM-GEOMAR
Leibniz-Institut für Meereswissenschaften
an der Universität Kiel

Das Leibniz-Institut für Meereswissenschaften
ist ein Institut der Wissenschaftsgemeinschaft
Gottfried Wilhelm Leibniz (WGL)

The Leibniz-Institute of Marine Sciences is a
member of the Leibniz Association
(Wissenschaftsgemeinschaft Gottfried
Wilhelm Leibniz).

Leibniz-Institut für Meereswissenschaften / Leibniz-Institute of Marine Sciences
IFM-GEOMAR
Dienstgebäude Westufer / West Shore Building
Düsternbrooker Weg 20
D-24105 Kiel
Germany

Leibniz-Institut für Meereswissenschaften / Leibniz-Institute of Marine Sciences
IFM-GEOMAR
Dienstgebäude Ostufer / East Shore Building
Wischhofstr. 1-3
D-24148 Kiel
Germany

Tel.: ++49 431 600-0
Fax: ++49 431 600-2805
www.ifm-geomar.de